

Noninvasive Adaptive Control of a Class of Nonlinear Systems With Unknown Parameters*

Hamed Rezaee[†] and Ludovic Renson[‡]

Abstract. Control-based continuation (CBC) is a general and systematic method to explore the dynamic response of a physical system and perform bifurcation analysis directly during experimental tests. Although CBC has been successfully demonstrated on a wide range of systems, rigorous and general approaches to designing a noninvasive controller underpinning the methodology are still lacking. In this paper, a noninvasive adaptive control strategy for a wide class of nonlinear systems with unknown parameters is proposed. We prove that the proposed adaptive control methodology is such that the states of the dynamical system track a reference signal in a noninvasive manner if and only if the reference is a response of the uncontrolled system to an excitation force. Compared to the existing literature, the proposed method does not require any a priori knowledge of some system parameters, does not require a persistent excitation, and is not restricted to linearly-stable systems, facilitating the application of CBC to a much larger class of systems than before. Rigorous mathematical analyses are provided, and the proposed control method is numerically demonstrated on a range of single- and multi-degree-of-freedom nonlinear systems, including a Duffing oscillator with multiple static equilibria. It is specifically shown that the unstable periodic orbits of the uncontrolled systems can be stabilized and reached, noninvasively, in controlled conditions.

Key words. Adaptive control, bi-stability, noninvasive control, nonlinear control, nonlinear dynamics, unstable periodic orbits.

MSC codes. 93C10, 93D21, 34C25, 37G15

1. Introduction. The general objective of a control system is to use the inputs of a dynamical system to lead state variables toward a desired value or trajectory. Noninvasive control refers to a particular class of control systems for which the control inputs asymptotically become zero if the states of the system approach responses of the underlying uncontrolled system. Despite vanishing, the controller can provide a stabilizing effect such that desired responses can be observed even if they correspond to unstable periodic orbits of the underlying uncontrolled system. An early application of this idea is chaos control where unstable periodic orbits embedded in a chaotic attractor are stabilized [49, 10]. In this context, numerous noninvasive control approaches have been developed such as the so-called OGY method [34, 41], time delayed feedback (TDF) [39, 16] and active filters [40, 30]. Chaos control has found applications in electronic circuits [40, 30], chemical oscillators [36, 38], lasers and nonlinear optics [6, 47], secure communication [22, 20], and fluid, mechanical, biological, and biochemical systems [54, 18]. More recent applications of noninvasive control use phase-locked loops (PLLs) to stabilize periodic oscillations in a range of mechanical systems [32, 21, 1, 13, 37].

More generally, noninvasive control provides a systematic means to explore the dynamics

*Submitted to the editors DATE.

Funding: This work was supported by the Engineering and Physical Sciences Research Council (EP/W032236/1).

[†]Department of Mechanical Engineering, Imperial College London, London, UK (h.rezaee@imperial.ac.uk).

[‡]Department of Mechanical Engineering, Imperial College London, London, UK (l.renson@imperial.ac.uk).

of a system purely based on its input-output relationship. The controller can be designed to steer the controlled dynamics toward responses described by a so-called reference signal. The noninvasive control inputs asymptotically vanish if the reference signal corresponds to a response of the uncontrolled system, which guarantees that the response is observed without affecting its position in state and parameter spaces. Finding a reference signal that results in vanishing control inputs defines a zero-problem whose solutions can be found iteratively and tracked in parameter space using suitable path-following techniques [48]. Control-based continuation (CBC) [53] exploits this idea for bifurcation analysis of physical systems directly during experiments. If properly designed, the control system can reduce (or even overcome) the sensitivity to initial conditions and stability changes due to bifurcations, which results in more repeatable experimental tests compared to traditional (uncontrolled) approaches. CBC has been used on a wide range of mechanical structures to measure important dynamics characteristics such as frequency response curves [4, 5, 11, 48, 24], backbone curves [43, 1], and fold bifurcation curves [45, 42]. More recently, CBC was used to characterize experimentally the equilibria of the Zeeman catastrophe machine [14], the dynamics of bubbles [17], the buckling of beams [33, 51, 52], and the limit cycle oscillations of an airfoil [25, 8], and demonstrated numerically on equilibria and periodic orbits in biological systems [12, 9]. Identified features can then be exploited for model development, calibration, and validation [25, 7, 55]. CBC contrasts with other noninvasive control methods like the OGY, TDF, and PLL in that it uses a reference signal. The reference signal acts as a proxy for the system states, which facilitates steering the system dynamics toward desired behaviors and exploring regions where multiple responses coexist. However, solving for the reference signal to achieve noninvasive control can be time-consuming, especially for slow-fast systems as investigated in [9].

Although CBC has been exploited in numerous studies, the majority of the existing literature primarily emphasizes its application rather than the systematic design and theoretical analysis of its underlying noninvasive control method. As such, new applications often require a significant number of trials and errors to obtain a controller that works throughout the parameter range of interest. In this paper, we contribute to filling this void by proposing a systematic noninvasive control strategy. Based on the idea of adaptive control, the gain/-parameters of the control system are not fixed. They will be adjusted under an adaptation strategy that guarantees the tracking of desired reference signals even if the parameters of the systems are unknown. The proposed control strategy addresses a wide class of high-order nonlinear systems with multiple degrees-of-freedom, and is designed such that the desired reference signal can be tracked in a noninvasive manner if and only if it is a response of the underlying uncontrolled system.

Recent work in this direction was presented in [35] where the design of noninvasive control using various techniques such as zero-in-equilibrium feedback control and washout filters was addressed. However, due to model nonlinearities and parameter uncertainties, achieving a desired tracking performance based on linear approaches may not be guaranteed. Accounting for model uncertainty, a noninvasive control method based on model-reference adaptive control and pole-placement adaptive control was proposed for linear discrete-time systems with periodic behavior in [27]. The approach was then extended to linear continuous-time systems with periodic behavior in [28] and to a class of nonlinear systems with periodic behavior in [29]. In [28] and [29], the linear terms of the system were assumed to be Hurwitz stable

and known. This helps design a model reference for a proper adaptive controller and guarantees stability. However, this assumption prevents the use of the controller in applications exhibiting multiple static equilibria (such as buckled beams and plates) and systems exhibiting self-excited oscillations (as in machine tool vibration, aeroelastic flutter, etc.). Another assumption made in [28] and [29] is that the desired response is persistently exciting. Based on such an assumption, the control input associated with a desired response should be rich enough (in terms of harmonic modes) to fully excite the dynamics of the system. Accordingly, it becomes possible to uniquely estimate the true unknown parameters of the system. This knowledge of the true parameters is then used in the controller to guarantee asymptotic tracking of the desired response together with the noninvasiveness of the control input. As shown in Section 5, satisfying this assumption is not always possible or may require a (very) fine discretization of the dynamics (using, for instance, a large number of Fourier modes), which increases the complexity and cost of solving the CBC root problem.

The control strategy proposed in the present paper lifts those assumptions such that no knowledge of any model parameter is needed, no stability assumptions are made on the linear terms of the system, and the performance of the proposed control strategy does not rely on the persistent excitation of the desired response. This makes our control method applicable to a much larger range of systems than before.

The structure of this paper is as follows. Notation is provided in the next section. Section 3 defines the noninvasive control problem in more precise terms, and the proposed noninvasive adaptive control method is presented in Section 4 along with rigorous proofs of its convergence and stability. In Section 5, simulation results on three different mechanical structures demonstrate the performance of the proposed control strategy, and Section 6 concludes this paper.

2. Notation. Throughout the paper \mathbb{R} and $\mathbb{R}_{>0}$ denote the set of real and positive real numbers, respectively. \mathbb{R}^n and $\mathbb{R}^{n \times m}$ denote the sets of $n \times 1$ real vectors and $n \times m$ real matrices, respectively. $v^{(k)}(t)$ denotes the k^{th} derivative of a variable $v(t)$. $\mathbf{0}_k$ is a $k \times 1$ vector of zeros. $|\cdot|$ denotes the absolute value. $\|\cdot\|$ denotes the 2-norm. $|\cdot|_\infty$ denotes the supremum value, and $\text{sat}(\cdot)$ denotes the saturation function, which for a scalar v , is defined as

$$\text{sat}(v/\epsilon) = \begin{cases} 1 & v \geq \epsilon \\ v/\epsilon & -\epsilon \leq v \leq \epsilon \\ -1 & v \leq -\epsilon, \end{cases}$$

where $\epsilon \in \mathbb{R}_{>0}$. Moreover, $\text{pol}(\lambda_i, k)$ is a polynomial of degree k with parameters $\lambda_i \in \mathbb{R}, i = 1, 2, \dots, k$, defined as $\text{pol}(\lambda_i, k) = s^k + \lambda_k s^{k-1} + \dots + \lambda_2 s + \lambda_1$.

3. Problem Statement. Consider a class of nonlinear systems with p degrees-of-freedom described as follows:

$$(3.1) \quad \begin{aligned} \mathbf{x}^{(n)}(t) &= \mathbf{F}(\boldsymbol{\xi}(t))\boldsymbol{\theta} + \mathbf{u}(t) \\ \boldsymbol{\xi} &= [\mathbf{x}^{(n-1)\top}(t) \quad \dots \quad \dot{\mathbf{x}}^\top(t) \quad \mathbf{x}^\top(t)]^\top, \end{aligned}$$

where $\mathbf{x}^{(k)}(t) \in \mathbb{R}^p, k \in \{0, 1, 2, \dots, n-1\}$, are the state vectors, $\mathbf{F}(\boldsymbol{\xi}(t)) \in \mathbb{R}^{p \times m}$ is a locally Lipschitz nonlinear function of the states which is known, $\boldsymbol{\theta} \in \mathbb{R}^m$ is a vector of unknown

constant parameters, and $\mathbf{u}(t) \in \mathbb{R}^n$ is the vector of inputs. This system can model a wide range of nonlinear systems that are linear in parameters (e.g., forced Duffing oscillators [2, 26], forced van der Pol oscillators [19, 31], aircraft attitude dynamics [46], and beam structures [44, 15]). System (3.1) considers identity input gains. The control method proposed here extends to systems with input gains in the form $\mathbf{B}\mathbf{u}(t)$ if \mathbf{B} is invertible and provided that \mathbf{B} can be identified a priori through tests. In such cases, the value of $\mathbf{u}(t)$ can be uniquely determined from $\mathbf{B}\mathbf{u}(t)$.

Assume that the bounded vector $\boldsymbol{\xi}^*(t) = [\mathbf{x}^{*(n-1)\top}(t) \ \dots \ \dot{\mathbf{x}}^{*\top}(t) \ \mathbf{x}^{*\top}(t)]^\top$ is a response of the system (3.1) to a harmonic force $\mathbf{u}(t) = \boldsymbol{\sigma}(t)$. Such responses also include equilibria and limit cycles when there is no excitation, i.e., when $\boldsymbol{\sigma}(t) = \mathbf{0}_n$. In an uncontrolled setting, various experiments for $\mathbf{u}(t) = \boldsymbol{\sigma}(t)$ but with different initial states may lead to different established responses and/or significantly different transient behaviors. In a controlled setting, it is possible to compensate for the effect of the initial conditions such that $\boldsymbol{\xi}(t)$ converges to a desired $\boldsymbol{\xi}^*(t)$ in a ‘reasonable’ time, and the control input simultaneously converges to zero, making the controller noninvasive.

Let us define $\mathbf{u}(t)$ as the combination of the external excitation $\boldsymbol{\sigma}(t)$ and a control input $\mathbf{u}'(t)$ as $\mathbf{u}(t) = \boldsymbol{\sigma}(t) + \mathbf{u}'(t)$. Since $\boldsymbol{\theta}$ is unknown, the objective is to propose an adaptive control strategy for the system (3.1) with a reference signal $\boldsymbol{\xi}^r(t) = [\mathbf{x}^{r(n-1)\top}(t) \ \dots \ \dot{\mathbf{x}}^{r\top}(t) \ \mathbf{x}^{r\top}(t)]^\top$, such that if $\boldsymbol{\xi}^r(t) = \boldsymbol{\xi}^*(t)$, the nonlinear system asymptotically converges to the following behavior:

$$(3.2) \quad \mathbf{x}^{*(n)}(t) = \mathbf{F}(\boldsymbol{\xi}^*(t))\boldsymbol{\theta} + \boldsymbol{\sigma}(t),$$

which implies that

$$(3.3) \quad \lim_{t \rightarrow \infty} (\boldsymbol{\xi}(t) - \boldsymbol{\xi}^*(t)) = \mathbf{0}_{np},$$

while the control input asymptotically converges to zero as follows:

$$\lim_{t \rightarrow \infty} \mathbf{u}'(t) = \mathbf{0}_p.$$

In the context of CBC, the response $\boldsymbol{\xi}^*(t)$ is a priori unknown and the reference signal $\boldsymbol{\xi}^r(t)$ should be iterated until the control input vanishes, implying that $\boldsymbol{\xi}^r(t) = \boldsymbol{\xi}^*(t)$. This defines a zero-problem whose solutions can be found using Newton-like methods and tracked in parameter space by using suitable path-following techniques [48, 45].

4. Noninvasive Adaptive Tracking Strategy. The proposed noninvasive control strategy is presented in this section. The main ideas underpinning the design are first presented before providing a theorem and the associated proof.

While noninvasive adaptive control of linear and nonlinear systems has already been addressed in the literature, partial knowledge of the system parameters and the persistently exciting nature of the responses were assumed [27, 28, 29]. In this context, the main achievements of the control method proposed here are to consider all the system parameters as unknown and to lift the persistent excitation requirement. To this end, the main idea of the proposed control strategy is to use the adaptive parameters for defining an auxiliary state.

This contrasts with the approach followed in [27, 28, 29] where adaptive parameters are directly used to define the control input. The proposed auxiliary state is designed in such a way that if it converges to a desired value, determined based on the desired response for the uncontrolled system, the real states of the system asymptotically converge to the desired response. Hence, our objective is to design a noninvasive control strategy such that the auxiliary state converges to its desired value, whereas the adaptive parameters may not converge to the real parameters of the system. Since the noninvasiveness of the control strategy does not rely on an exact estimation of the unknown parameters, the desired response is not required to be persistently exciting.

Let us consider the following auxiliary state:

$$(4.1) \quad \mathbf{z}(t) = \mathbf{x}^{(n-1)}(t) - \int_0^t \left(\mathbf{F}(\boldsymbol{\xi}(\tau)) \hat{\boldsymbol{\theta}}(\tau) + \boldsymbol{\sigma}(\tau) + \boldsymbol{\eta}(\tau) \right) d\tau,$$

where $\hat{\boldsymbol{\theta}}(t) \in \mathbb{R}^m$ are the adaptive parameters and $\boldsymbol{\eta}(t) \in \mathbb{R}^p$ is a control law. We recall that the reference states $\boldsymbol{\xi}^*(t)$ satisfy (3.2), which implies that

$$(4.2) \quad \mathbf{x}^{*(n-1)}(0) = \mathbf{x}^{*(n-1)}(t) - \int_0^t \left(\mathbf{F}(\boldsymbol{\xi}^*(\tau)) \boldsymbol{\theta} + \boldsymbol{\sigma}(\tau) \right) d\tau.$$

Observing the similarity between (4.1) and (4.2), if we design the control strategy with the reference signal $\boldsymbol{\xi}^r(t)$ such that $\mathbf{z}(t)$ converges to $\mathbf{x}^{*(n-1)}(0)$, the dynamics of the state $\mathbf{x}^{(n-1)}(t)$ converges to that of $\mathbf{x}^{*(n-1)}(t)$. Given that $\mathbf{x}^{(n-1)}(t)$ stands for the states with the highest derivative, this does not guarantee the convergence of the other states. Hence, we should also design $\boldsymbol{\eta}(t)$ such that $\mathbf{x}(t)$ and its derivatives converge to $\mathbf{x}^*(t)$ and its derivatives, respectively, and the objective (3.3) is achieved. Moreover, the parameter adaption law is designed as

$$(4.3) \quad \dot{\hat{\boldsymbol{\theta}}}(t) = \mathbf{S} \mathbf{F}(\boldsymbol{\xi}(t))^\top (\mathbf{z}(t) - \mathbf{x}^{r(n-1)}(0)),$$

where $\mathbf{S} \in \mathbb{R}^{m \times m}$ is symmetric positive definite. Now, based on the definition of $\mathbf{z}(t)$, the control input $\mathbf{u}'(t)$ is designed as

$$(4.4) \quad \mathbf{u}'(t) = \boldsymbol{\eta}(t) - k(\mathbf{z}(t) - \mathbf{x}^{r(n-1)}(0)),$$

where $k \in \mathbb{R}_{>0}$. According to (4.4), if $\mathbf{z}(t)$ converges to $\mathbf{x}^{r(n-1)}(0)$, $\mathbf{u}'(t)$ is noninvasive if $\boldsymbol{\eta}(t)$ becomes noninvasive as (3.3) is reached. Accordingly, we design $\boldsymbol{\eta}(t)$ as follows:

$$(4.5) \quad \boldsymbol{\eta}(t) = -\lambda_{n-1} \mathbf{e}^{(n-1)}(t) - \dots - \lambda_1 \dot{\mathbf{e}}(t) - \phi(t) \mathbf{y}(t) - g(\boldsymbol{\xi}(t), \boldsymbol{\xi}^r(t), \hat{\boldsymbol{\theta}}(t)) \text{sat}(\mathbf{y}(t)/\epsilon),$$

where $\mathbf{e}(t) = \mathbf{x}(t) - \mathbf{x}^r(t)$ denotes the tracking error, the coefficients $\lambda_i \in \mathbb{R}_{>0}$, $i \in \{1, 2, \dots, n-1\}$, are such that the polynomial $\text{pol}(\lambda_i, n-1)$ is Hurwitz stable, and $\mathbf{y}(t)$ is as follows:

$$(4.6) \quad \mathbf{y}(t) = \mathbf{e}^{(n-1)}(t) + \lambda_{n-1} \mathbf{e}^{(n-2)}(t) + \dots + \lambda_1 \mathbf{e}(t).$$

Since $\text{pol}(\lambda_i, n-1)$ is Hurwitz stable, if we show the convergence of $\mathbf{y}(t)$ to zero, the tracking error $\mathbf{e}(t)$ and its derivatives, $\mathbf{e}^{(k)}(t)$, $k \in \{1, 2, \dots, n-1\}$, converge to zero as well. The benefit in defining $\mathbf{y}(t)$ is to control just one vector instead of controlling n vectors $\mathbf{e}^{(k)}(t)$, $k \in$

$\{0, 1, \dots, n-1\}$, simplifying the design and analysis of the control strategy in the rest of the paper. Moreover, $\phi(t) \in \mathbb{R}$ is a time-varying parameter updated as follows:

$$(4.7) \quad \dot{\phi}(t) = \gamma \mathbf{y}^\top(t) \mathbf{y}(t),$$

with $\gamma \in \mathbb{R}_{>0}$, and $g(\boldsymbol{\xi}(t), \boldsymbol{\xi}^r(t), \hat{\boldsymbol{\theta}}(t))$ is a control gain considered as

$$(4.8) \quad g(\boldsymbol{\xi}(t), \boldsymbol{\xi}^r(t), \hat{\boldsymbol{\theta}}(t)) = \|(\mathbf{F}(\boldsymbol{\xi}(t)) - \mathbf{F}(\boldsymbol{\xi}^r(t)))\hat{\boldsymbol{\theta}}(t)\| + \kappa,$$

with $\kappa \in \mathbb{R}_{>0}$. The main objective behind the definition of $\boldsymbol{\eta}(t)$ as (4.5) is to guarantee the boundedness of the states of the controlled system along with the convergence of $\mathbf{y}(t)$ to zero, which is discussed in detail in the next theorem.

Remark 4.1. It should be noted that in the standard adaptive control, the term $\mathbf{F}(\boldsymbol{\xi}(t))\hat{\boldsymbol{\theta}}(t)$ will be used in the control input. Hence, if $\hat{\boldsymbol{\theta}}(t)$ converges to $\boldsymbol{\theta}(t)$ (in the case of persistent excitation), the term $-\mathbf{F}(\boldsymbol{\xi}(t))\hat{\boldsymbol{\theta}}(t)$ in the controller compensates for the unknown nonlinear term $\mathbf{F}(\boldsymbol{\xi}(t))\boldsymbol{\theta}$. Therefore, the noninvasiveness of the control input can be guaranteed by tracking a reference $\boldsymbol{\xi}^r(t)$. However, this persistent excitation condition can be difficult to satisfy. In this paper, according to (4.4) and (4.5), the term $\mathbf{F}(\boldsymbol{\xi}(t))\hat{\boldsymbol{\theta}}(t)$ is not directly used as an additive term in the control input. Hence, it is not necessary for $\hat{\boldsymbol{\theta}}(t)$ to converge to the true parameters $\boldsymbol{\theta}(t)$, and therefore the persistent excitation is not required. Such a term appears only in the gain $g(\boldsymbol{\xi}(t), \boldsymbol{\xi}^r(t), \hat{\boldsymbol{\theta}}(t))$ in front of $\text{sat}(\mathbf{y}(t)/\epsilon)$ and not directly as an additive term in $\mathbf{u}'(t)$. As such, the term $g(\boldsymbol{\xi}(t), \boldsymbol{\xi}^r(t), \hat{\boldsymbol{\theta}}(t))\text{sat}(\mathbf{y}(t)/\epsilon)$ converges to zero if we guarantee that $\mathbf{y}(t)$ converges to zero. As a result, whether $\hat{\boldsymbol{\theta}}(t)$ converges to $\boldsymbol{\theta}(t)$ or not, the noninvasiveness of the control input can still be guaranteed.

Theorem 4.2. *Consider the nonlinear system (3.1) with responses $\boldsymbol{\xi}^*(t)$ to the excitation force $\boldsymbol{\sigma}(t)$. Let $\mathbf{u}(t) = \boldsymbol{\sigma}(t) + \mathbf{u}'(t)$ where $\mathbf{u}'(t)$ is the control strategy defined in (4.4) with a bounded smooth reference signal $\boldsymbol{\xi}^r(t)$. Under this condition, if $\boldsymbol{\xi}^r(t) = \boldsymbol{\xi}^*(t)$,*

$$(4.9) \quad \lim_{t \rightarrow \infty} (\boldsymbol{\xi}(t) - \boldsymbol{\xi}^*(t)) = \mathbf{0}_{np},$$

while $\mathbf{u}'(t)$ is bounded and noninvasive. Moreover, if $\boldsymbol{\xi}^r(t)$ is not a response of the system to $\boldsymbol{\sigma}(t)$; then, while $\boldsymbol{\xi}(t)$ remains bounded, it does not converge to $\boldsymbol{\xi}^r(t)$, and a stable equilibrium of the tracking error system implies nonzero control input.

Proof. The proof of the theorem is presented in two parts. In the first part we consider the case when $\boldsymbol{\xi}^r(t) = \boldsymbol{\xi}^*(t)$, and in the second part the case when $\boldsymbol{\xi}^r(t)$ is not a response of the system to $\boldsymbol{\sigma}(t)$ is considered.

Part 1: We prove the first part of the theorem in two steps. In the first step, we show that for $\boldsymbol{\xi}^r(t) = \boldsymbol{\xi}^*(t)$, $\mathbf{z}(t)$ remains bounded and converges to $\mathbf{x}^{*(n-1)}(0)$, and $\hat{\boldsymbol{\theta}}(t)$, $\boldsymbol{\xi}(t)$, $\mathbf{F}(\boldsymbol{\xi}(t))$, and $\dot{\mathbf{z}}(t)$ remain bounded. Then, in the next step, the achievement of the objective (4.9) along with the boundedness of $\phi(t)$ is investigated. Then, we conclude that $\mathbf{u}'(t)$ remains bounded and converges to zero.

Step 1—By considering the definition of $\mathbf{z}(t)$ in (4.1) and since $\mathbf{u}(t) = \boldsymbol{\sigma}(t) + \mathbf{u}'(t)$, along (3.1) one gets

$$(4.10) \quad \dot{\mathbf{z}}(t) = \mathbf{F}(\boldsymbol{\xi}(t))\boldsymbol{\theta} + \mathbf{u}'(t) - \mathbf{F}(\boldsymbol{\xi}(t))\hat{\boldsymbol{\theta}}(t) - \boldsymbol{\eta}(t).$$

To analyze (4.10) under the control law (4.4), we consider the following Lyapunov candidate:

$$(4.11) \quad V(t) = \frac{1}{2} \tilde{\mathbf{z}}^\top(t) \tilde{\mathbf{z}}(t) + \frac{1}{2} \tilde{\boldsymbol{\theta}}^\top(t) \mathbf{S}^{-1} \tilde{\boldsymbol{\theta}}(t),$$

where $\tilde{\mathbf{z}}(t) = \mathbf{z}(t) - \mathbf{x}^{r(n-1)}(0)$ and $\tilde{\boldsymbol{\theta}}(t) = \hat{\boldsymbol{\theta}}(t) - \boldsymbol{\theta}$. Since $\boldsymbol{\theta}$ is constant, the time-derivation of $V(t)$ along (4.3), (4.4), and (4.10), after some simplification yields

$$(4.12) \quad \dot{V}(t) = -k \tilde{\mathbf{z}}^\top(t) \tilde{\mathbf{z}}(t).$$

From (4.11) and (4.12), it follows that $\tilde{\mathbf{z}}(t)$, $\mathbf{z}(t)$, $\tilde{\boldsymbol{\theta}}(t)$, and $\hat{\boldsymbol{\theta}}(t)$ remain bounded. Since $\boldsymbol{\xi}^r(t) = \boldsymbol{\xi}^*(t)$, by considering (4.1) and (4.2) and according to the definition of $\mathbf{e}(t)$, one gets

$$(4.13) \quad \tilde{\mathbf{z}}(t) = \mathbf{e}^{(n-1)}(t) - \int_0^t \left(\mathbf{F}(\boldsymbol{\xi}^r(\tau)) \hat{\boldsymbol{\theta}}(\tau) - \mathbf{F}(\boldsymbol{\xi}^r(\tau)) \boldsymbol{\theta} + \boldsymbol{\eta}(\tau) \right) d\tau.$$

By adding and subtracting $\int_0^t \mathbf{F}(\boldsymbol{\xi}^r(\tau)) \hat{\boldsymbol{\theta}}(\tau) d\tau$ to the right hand side of (4.13) and according to the definition of $\tilde{\boldsymbol{\theta}}(t)$, one observes that

$$(4.14) \quad \tilde{\mathbf{z}}(t) = \mathbf{e}^{(n-1)}(t) - \int_0^t \left(\mathbf{F}(\boldsymbol{\xi}^r(\tau)) \tilde{\boldsymbol{\theta}}(\tau) + (\mathbf{F}(\boldsymbol{\xi}(\tau)) - \mathbf{F}(\boldsymbol{\xi}^r(\tau))) \hat{\boldsymbol{\theta}}(\tau) + \boldsymbol{\eta}(\tau) \right) d\tau.$$

By substituting $\boldsymbol{\eta}(t)$ defined in (4.5) into (4.14), and according to the definition of $\mathbf{y}(t)$ in (4.6) one gets

$$(4.15) \quad \begin{aligned} \tilde{\mathbf{z}}(t) = & \mathbf{y}(t) - \int_0^t \left(\mathbf{F}(\boldsymbol{\xi}^r(\tau)) \tilde{\boldsymbol{\theta}}(\tau) + (\mathbf{F}(\boldsymbol{\xi}(\tau)) - \mathbf{F}(\boldsymbol{\xi}^r(\tau))) \hat{\boldsymbol{\theta}}(\tau) - \phi(\tau) \mathbf{y}(\tau) \right. \\ & \left. - g(\boldsymbol{\xi}(\tau), \boldsymbol{\xi}^r(\tau), \hat{\boldsymbol{\theta}}(\tau)) \text{sat}(\mathbf{y}(\tau)/\epsilon) \right) d\tau - \lambda_{n-1} \mathbf{e}^{(n-2)}(0) - \dots - \lambda_1 \mathbf{e}(0). \end{aligned}$$

Now, by decomposing the $\mathbf{y}(t)$ into its p entries as

$$\mathbf{y}(t) = [y_1(t) \quad y_2(t) \quad \dots \quad y_p(t)]^\top,$$

we consider two cases. The first is when $|y_k(t)| \leq \epsilon, \forall k \in \{1, 2, \dots, p\}$, and the second is when $|y_k(t)| > \epsilon$ for some $k \in \{1, 2, \dots, p\}$. These two cases are discussed below:

Case 1: If $|y_k(t)| \leq \epsilon, \forall k \in \{1, 2, \dots, p\}$, according to the definition of $\mathbf{y}(t)$ in (4.6) and since the polynomial $\text{pol}(\lambda_i, n-1)$ is Hurwitz stable, $\mathbf{e}^{(k)}(t), k \in \{0, 1, \dots, n-1\}$, are bounded (due to input-to-state stability of Hurwitz linear systems [23]). In this condition, since $\boldsymbol{\xi}^r(t) = [\mathbf{x}^{r(n-1)\top}(t) \quad \dots \quad \dot{\mathbf{x}}^{r\top}(t) \quad \mathbf{x}^{r\top}(t)]^\top$ is bounded, $\boldsymbol{\xi}(t) = [\mathbf{x}^{(n-1)\top}(t) \quad \dots \quad \dot{\mathbf{x}}^\top(t) \quad \mathbf{x}^\top(t)]^\top$ is bounded as well. Then, as $\mathbf{F}(\cdot)$ is a locally Lipschitz function, the boundedness of $\boldsymbol{\xi}(t)$ implies the boundedness of $\mathbf{F}(\boldsymbol{\xi}(t))$. By considering (4.4) and (4.10), we have

$$(4.16) \quad \dot{\mathbf{z}}(t) = \mathbf{F}(\boldsymbol{\xi}(t)) \boldsymbol{\theta} - k \tilde{\mathbf{z}}(t) - \mathbf{F}(\boldsymbol{\xi}(t)) \hat{\boldsymbol{\theta}}(t).$$

Hence, as $\mathbf{F}(\boldsymbol{\xi}(t))$, $\hat{\boldsymbol{\theta}}(t)$, and $\tilde{\mathbf{z}}(t)$ are bounded, from (4.16) the boundedness of $\dot{\mathbf{z}}(t)$ can be concluded.

Case 2: If there exist $k \in \{1, 2, \dots, p\}$ such that $|y_k(t)| > \epsilon$, according to the definition of the saturation function, $\text{sat}(y_k(t)/\epsilon) = y_k(t)/|y_k(t)|$. Let us decompose $(\mathbf{F}(\boldsymbol{\xi}(t)) - \mathbf{F}(\boldsymbol{\xi}^r(t)))\hat{\boldsymbol{\theta}}(t)$ to p entries as follows:

$$(\mathbf{F}(\boldsymbol{\xi}(t)) - \mathbf{F}(\boldsymbol{\xi}^r(t)))\hat{\boldsymbol{\theta}}(t) = [\mathfrak{F}_1(t) \quad \mathfrak{F}_2(t) \quad \dots \quad \mathfrak{F}_p(t)]^\top.$$

By considering (4.8) and according to the definition of $\mathfrak{F}_k(t)$, $\text{sat}(y_k(t)/\epsilon) = y_k(t)/|y_k(t)|$ implies that there exists $\beta_k(t) \in \mathbb{R}_{>0}$, such that

$$(4.17) \quad -\mathfrak{F}_k(t) + g(\boldsymbol{\xi}(t), \boldsymbol{\xi}^r(t), \hat{\boldsymbol{\theta}}(t))\text{sat}(y_k(t)/\epsilon) = \beta_k(t)y_k(t).$$

Now, let us decompose $\tilde{\mathbf{z}}(t)$, $\mathbf{F}(\boldsymbol{\xi}^r(t))\tilde{\boldsymbol{\theta}}(t)$, and $\mathbf{e}(t)$ as follows:

$$\begin{aligned} \tilde{\mathbf{z}}(t) &= [\tilde{z}_1(t) \quad \tilde{z}_2(t) \quad \dots \quad \tilde{z}_p(t)]^\top \\ \mathbf{F}(\boldsymbol{\xi}^r(t))\tilde{\boldsymbol{\theta}}(t) &= [\mathfrak{F}'_1(t) \quad \mathfrak{F}'_2(t) \quad \dots \quad \mathfrak{F}'_p(t)]^\top \\ \mathbf{e}(t) &= [e_1(t) \quad e_2(t) \quad \dots \quad e_p(t)]^\top. \end{aligned}$$

By considering (4.17), from (4.15) one gets

$$(4.18) \quad \begin{aligned} y_k(t) &= \int_0^t \left(\mathfrak{F}'_k(\tau) - \beta_k(\tau)y_k(\tau) - \phi(\tau)y_k(\tau) \right) d\tau \\ &+ \lambda_{n-1}e_k^{(n-2)}(0) + \dots + \lambda_1 e_k(0) + \tilde{z}_k(t). \end{aligned}$$

Since $\mathfrak{F}'_k(t)$ and $\tilde{z}_k(t)$ are bounded and $\beta_k(t) + \phi(t)$ is positive, by considering (4.18), it follows that $y_k(t)$ remains bounded. Hence, based on the arguments given for Case 1, the boundedness of $\boldsymbol{\xi}(t)$ and $\mathbf{F}(\boldsymbol{\xi}(t))$ and then the boundedness of $\dot{\mathbf{z}}(t)$ can be concluded.

According to the aforementioned two cases, $\boldsymbol{\xi}(t)$, $\mathbf{F}(\boldsymbol{\xi}(t))$, and $\dot{\mathbf{z}}(t)$ are bounded. By considering (4.12), $\dot{V}(t)$ is negative semidefinite. Since $V(t)$ is lower bounded and $\dot{V}(t)$ is nonpositive, the limit of $V(t)$ exists, and $V(t)$ converges to a constant value. The convergence of $V(t)$ to a constant value means that the integration of $\dot{V}(t)$ over any finite period of time should converge to zero. In other words, in the time period $[t, t+s]$, $t \rightarrow \infty$, for any real positive constant s , we should have

$$(4.19) \quad \lim_{t \rightarrow \infty} \int_t^{t+s} \dot{V}(\tau) d\tau = 0.$$

Equation (4.19) means that $\dot{V}(t)$ converges to zero in the time period $[t, t+s]$, $t \rightarrow \infty$, unless $\ddot{V}(t)$ is unbounded for bounded $\dot{V}(t)$, but such discontinuity is not possible according to (4.16) (this can be also concluded by the Barbalat lemma [56] and the invariance principle for nonautonomous systems [3]). Therefore, $\dot{V}(t)$ converges to zero which implies that $\tilde{\mathbf{z}}(t)$ converges to zero.

Step 2–From (4.15) one gets

$$(4.20) \quad \begin{aligned} \dot{\mathbf{y}}(t) &= (\mathbf{F}(\boldsymbol{\xi}(t)) - \mathbf{F}(\boldsymbol{\xi}^r(t)))\hat{\boldsymbol{\theta}} - \phi(t)\mathbf{y}(t) - g(\boldsymbol{\xi}(t), \boldsymbol{\xi}^r(t), \hat{\boldsymbol{\theta}}(t))\text{sat}(\mathbf{y}(t)/\epsilon) \\ &+ \dot{\mathbf{z}}(t) + \mathbf{F}(\boldsymbol{\xi}^r(t))\tilde{\boldsymbol{\theta}}(t). \end{aligned}$$

Since $\tilde{z}(t)$ converges to zero, for any $s \in \mathbb{R}_{>0}$,

$$(4.21) \quad \lim_{t \rightarrow \infty} \int_t^{t+s} \dot{z}(\tau) d\tau = 0.$$

Equation (4.21) means that $\dot{z}(t)$ converges to zero in the time period $[t, t+s]$, $t \rightarrow \infty$, unless $\dot{z}(t)$ is unbounded for bounded $z(t)$, but such discontinuity is not possible according to the nonlinear system (4.16). Hence, the convergence of $\dot{z}(t)$ to zero can be concluded. Since $\dot{z}(t)$ and $\tilde{z}(t)$ remain bounded and converge to zero, from (4.16) it follows that $\mathbf{F}(\boldsymbol{\xi}(t))\tilde{\boldsymbol{\theta}}(t)$ remains bounded and converges to zero. By adding and subtracting $\mathbf{F}(\boldsymbol{\xi}(t))\tilde{\boldsymbol{\theta}}(t)$ to the right side of (4.20) and since $\tilde{\boldsymbol{\theta}}(t) = \hat{\boldsymbol{\theta}}(t) - \boldsymbol{\theta}$, after some manipulation one gets

$$(4.22) \quad \dot{\mathbf{y}}(t) = (\mathbf{F}(\boldsymbol{\xi}(t)) - \mathbf{F}(\boldsymbol{\xi}^r(t)))\boldsymbol{\theta} - \phi(t)\mathbf{y}(t) - g(\boldsymbol{\xi}(t), \boldsymbol{\xi}^r(t), \hat{\boldsymbol{\theta}}(t))\text{sat}(\mathbf{y}(t)/\epsilon) + \mathbf{w}(t),$$

where $\mathbf{w}(t) = \dot{z}(t) + \mathbf{F}(\boldsymbol{\xi}(t))\tilde{\boldsymbol{\theta}}(t)$ is bounded and converges to zero. As $\boldsymbol{\xi}(t)$ and $\boldsymbol{\xi}^r(t)$ are bounded and $\mathbf{F}(\cdot)$ is locally Lipschitz, there exists a finite constant $\ell_1 \in \mathbb{R}_{>0}$ such that

$$(4.23) \quad \|\mathbf{F}(\boldsymbol{\xi}(t)) - \mathbf{F}(\boldsymbol{\xi}^r(t))\| \leq \ell_1 \|\boldsymbol{\xi}(t) - \boldsymbol{\xi}^r(t)\|.$$

Moreover, according to (4.6), since the polynomial $\text{pol}(\lambda_i, n-1)$ is Hurwitz stable, there exists a vanishing bounded function $h(t, \mathbf{e}(0), \dots, \mathbf{e}^{(n-2)}(0))$ and a finite constant $\ell_2 \in \mathbb{R}_{>0}$ such that [23]

$$(4.24) \quad \|\boldsymbol{\xi}(t) - \boldsymbol{\xi}^r(t)\| \leq h + \ell_2 \|\mathbf{y}(t)\|.$$

Hence, by considering (4.23) and (4.24), one gets

$$(4.25) \quad \|\mathbf{F}(\boldsymbol{\xi}(t)) - \mathbf{F}(\boldsymbol{\xi}^r(t))\| \leq \ell_1 h + \ell_1 \ell_2 \|\mathbf{y}(t)\|.$$

Now, we consider the following Lyapunov candidate:

$$V'(t) = \frac{1}{2} \mathbf{y}^\top(t) \mathbf{y}(t) + \frac{1}{2} \gamma^{-1} (\phi(t) - \phi^*)^2,$$

where $\phi^* \in \mathbb{R}_{>0}$ is a constant that satisfies the following inequality for an arbitrary $\varrho \in \mathbb{R}_{>0}$,

$$(4.26) \quad \phi^* > \frac{\varrho}{2} + \ell_1 \ell_2 \|\boldsymbol{\theta}\|.$$

The time derivation of $V'(t)$ along (4.7) and (4.22) yields

$$(4.27) \quad \begin{aligned} \dot{V}'(t) &= \mathbf{y}^\top(t) (\mathbf{F}(\boldsymbol{\xi}(t)) - \mathbf{F}(\boldsymbol{\xi}^r(t)))\boldsymbol{\theta} - \phi(t)\mathbf{y}^\top(t)\mathbf{y}(t) - g(\boldsymbol{\xi}(t), \boldsymbol{\xi}^r(t), \hat{\boldsymbol{\theta}}(t))\mathbf{y}^\top(t)\text{sat}(\mathbf{y}(t)/\epsilon) \\ &+ \mathbf{y}^\top(t)\mathbf{w}(t) + (\phi(t) - \phi^*)\mathbf{y}^\top(t)\mathbf{y}(t). \end{aligned}$$

According to the Young inequality, one observes that

$$(4.28) \quad \mathbf{y}^\top(t)\mathbf{w}(t) \leq \frac{\varrho}{2} \mathbf{y}^\top(t)\mathbf{y}(t) + \frac{1}{2\varrho} \mathbf{w}^\top(t)\mathbf{w}(t).$$

By considering (4.25) and (4.28), (4.27) can be simplified as follows:

$$(4.29) \quad \dot{V}'(t) \leq \ell_1 h \|\boldsymbol{\theta}\| \|\mathbf{y}(t)\| + \ell_1 \ell_2 \|\boldsymbol{\theta}\| \mathbf{y}^\top(t) \mathbf{y}(t) + \frac{\rho}{2} \mathbf{y}^\top(t) \mathbf{y}(t) + \frac{1}{2\rho} \mathbf{w}^\top(t) \mathbf{w}(t) - \phi^* \mathbf{y}^\top(t) \mathbf{y}(t),$$

where $\ell_1 h \|\boldsymbol{\theta}\| \|\mathbf{y}(t)\|$ is bounded and converges to zero. Note that as $\boldsymbol{\xi}(t)$ and $\boldsymbol{\xi}^r(t)$ are bounded, $\mathbf{y}(t)$ is also bounded. From (4.26) and (4.29), it follows that there exists $\chi \in \mathbb{R}_{>0}$ such that

$$(4.30) \quad \dot{V}'(t) \leq -\chi \mathbf{y}^\top(t) \mathbf{y}(t) + \ell_1 h \|\boldsymbol{\theta}\| \|\mathbf{y}(t)\| + \frac{1}{2\rho} \mathbf{w}^\top(t) \mathbf{w}(t).$$

Since $\ell_1 h \|\boldsymbol{\theta}\| \|\mathbf{y}(t)\| + 1/(2\rho) \mathbf{w}^\top(t) \mathbf{w}(t)$ is bounded and converges to zero, according to (4.30), for any nonzero $\mathbf{y}(t)$ there exists a finite time t_f such that for $t \geq t_f$, $\dot{V}'(t)$ is negative semidefinite. Note that according to (4.7) and (4.22), $V'(t)$ cannot become unbounded in finite time. Therefore, as $\dot{V}'(t)$ is negative semidefinite for $t \geq t_f$, $V'(t)$ is bounded at all times. Hence, the limit of $V'(t)$ exists, that is, for any $s \in \mathbb{R}_{>0}$,

$$(4.31) \quad \lim_{t \rightarrow \infty} \int_t^{t+s} \dot{V}'(\tau) d\tau = 0.$$

Equation (4.31) means that $\dot{V}'(t)$ converges to zero in the time period $[t, t+s], t \rightarrow \infty$, unless $\dot{V}'(t)$ is unbounded for bounded $V'(t)$ which is not possible according to (4.7) and (4.22). Hence, $\dot{V}'(t)$ converges to zero which implies that $\mathbf{y}(t)$ converges to zero. According to (4.6), by convergence of $\mathbf{y}(t)$ to zero, since the polynomial $\text{pol}(\lambda_i, n-1)$ is Hurwitz stable, $\mathbf{e}^{(k)}(t), k \in \{0, 1, \dots, n-1\}$, converge to zero. Therefore, the objective (4.9) is satisfied. Moreover, since $V'(t)$ is bounded, $\phi(t)$ remains bounded. Hence, as $\mathbf{y}(t)$ and $\boldsymbol{\xi}(t)$ are bounded, $\mathbf{u}'(t)$ is bounded. Now, we need to show that $\mathbf{u}'(t)$ converges to zero. We have shown that $\mathbf{e}^{(k)}(t), k \in \{0, 1, \dots, n-1\}$, and $\mathbf{y}(t)$ converge to zero. It was also shown that $\tilde{\mathbf{z}}(t)$ converges to zero. Therefore, according to (4.4) and (4.5), $\mathbf{u}'(t)$ converges to zero.

Part 2: If $\boldsymbol{\xi}^r(t)$ is not a response of the system to $\boldsymbol{\sigma}(t)$, from (3.2) it follows that

$$(4.32) \quad \mathbf{x}^{r(n)}(t) = \mathbf{F}(\boldsymbol{\xi}^r(t)) \boldsymbol{\theta} + \boldsymbol{\sigma}(t) + \boldsymbol{\Delta}(t),$$

where $\boldsymbol{\Delta}(t) \in \mathbb{R}^p$ is bounded and not identical to zero. According to (4.32), one gets

$$(4.33) \quad \mathbf{x}^{r(n-1)}(0) = \mathbf{x}^{r(n-1)}(t) - \int_0^t \left(\mathbf{F}(\boldsymbol{\xi}^r(\tau)) \boldsymbol{\theta} + \boldsymbol{\Delta}(\tau) + \boldsymbol{\sigma}(\tau) \right) d\tau.$$

In Part 1, it was show that if $|y_k(t)| \leq \epsilon, \forall k \in \{1, 2, \dots, p\}$, $\boldsymbol{\xi}(t)$ always remains bounded. Let us now consider the case when $|y_k(t)| > \epsilon$ for some $k \in \{1, 2, \dots, p\}$. By decomposing $\boldsymbol{\Delta}(t)$ as

$$\boldsymbol{\Delta}(t) = [\Delta_1(t) \quad \Delta_2(t) \quad \dots \quad \Delta_p(t)]^\top,$$

and by considering (4.33), (4.18) yields

$$(4.34) \quad \begin{aligned} \tilde{z}_k(t) &= y_k(t) - \int_0^t \left(\mathfrak{F}'_k(\tau) - \beta_k(\tau) y_k(\tau) - \phi(\tau) y_k(\tau) - \Delta_k(\tau) \right) d\tau \\ &\quad - \lambda_{n-1} e_k^{(n-2)}(0) - \dots - \lambda_1 e_k(0). \end{aligned}$$

Note that whether $\Delta(t)$ is identical to zero or not, (4.12) still is satisfied, implying that $\tilde{z}(t)$ and $\tilde{\theta}(t)$ are bounded, and hence $\tilde{z}_k(t)$ and $\tilde{\mathfrak{F}}'_k(t)$ are bounded. Since $\tilde{z}_k(t)$, $\tilde{\mathfrak{F}}'_k(t)$, and $\Delta_k(t)$ are bounded and $\beta_k(t) + \phi(t)$ is positive, by considering (4.34), $y_k(t)$ remains bounded. Hence, the boundedness of $\xi(t)$ can be concluded. By considering (4.33), (4.22) also becomes

$$(4.35) \quad \begin{aligned} \dot{\mathbf{y}}(t) &= (\mathbf{F}(\xi(t)) - \mathbf{F}(\xi^r(t)))\boldsymbol{\theta} - \phi(t)\mathbf{y}(t) - g(\xi(t), \xi^r(t), \hat{\boldsymbol{\theta}}(t))\text{sat}(\mathbf{y}(t)/\epsilon) \\ &\quad - \Delta(t) + \mathbf{w}(t). \end{aligned}$$

Whether $\Delta(t)$ is identical to zero or not, in a way similar to Part 1, one observes that $\tilde{z}(t)$, $\dot{z}(t)$ and then $\mathbf{w}(t)$ converge to zero. Therefore, if $\Delta(t)$ is not identical to zero, $\mathbf{y}(t) = \mathbf{0}_p$ is not the equilibrium point of the system (4.35). Hence, $\mathbf{e}(t)$ does not converge to zero. Moreover, since $\xi^r(t)$ is not a response of the system to $\boldsymbol{\sigma}(t)$, (3.2) cannot be satisfied for the system (3.1). Therefore, as $\mathbf{u}(t) = \boldsymbol{\sigma}(t) + \mathbf{u}'(t)$, $\mathbf{u}'(t) = \mathbf{0}_p$ does not imply a stable equilibrium for the tracking error system, that is, a stable equilibrium of the tracking error system implies nonzero control input. ■

According to the results of Theorem 4.2, if the reference signal $\xi^r(t)$ is a response of the system (3.1) to the excitation force $\boldsymbol{\sigma}(t)$, $\xi(t)$ converges to $\xi^r(t)$, while $\mathbf{u}'(t)$ is noninvasive. In the context of CBC, the behavior of the uncontrolled system is a priori unknown. Hence, to discover such uncontrolled behavior, the reference signal $\xi^r(t)$ will be found iteratively by checking whether it makes the control input noninvasive or not. Hence, as addressed in Theorem 4.2, it is desirable to guarantee that the reference signal results in noninvasive control “only if” it is a response of the nonlinear system (3.1) to $\boldsymbol{\sigma}(t)$. In other words, in cases when the reference $\xi^r(t)$ is not a response of the system (3.1) to $\boldsymbol{\sigma}(t)$, $\xi(t)$ should not converge to $\xi^r(t)$ and $\mathbf{u}'(t)$ should be invasive. The obtained results are validated by numerical simulation in the next section.

Remark 4.3. According to the proof of Theorem 4.2, while the proposed control strategy relies on the adaptive vector $\hat{\boldsymbol{\theta}}(t)$, the convergence of $\hat{\boldsymbol{\theta}}(t)$ to the real system parameters $\boldsymbol{\theta}$ is not required. Accordingly, the persistent excitation of $\xi^*(t)$, which is typically required for $\hat{\boldsymbol{\theta}}(t)$ to converge to $\boldsymbol{\theta}$, is not a condition for the accurate performance of the proposed control strategy. However, if $\xi^*(t)$ is persistently exciting, it is straightforward to show that under the proposed control strategy, while tracking $\xi^*(t)$, $\hat{\boldsymbol{\theta}}(t)$ asymptotically converges to $\boldsymbol{\theta}$.

Remark 4.4. The control strategy proposed in (4.1)-(4.8) is leading the system behavior toward the surface $\mathbf{y}(t) = \mathbf{0}_p$, which according to (4.6) implies that the system is controlled by a linear controller. Taking a second-order dynamical system as an example, the behavior of the system on $\mathbf{y}(t) = \mathbf{0}_p$ is thus similar to a system controlled by a proportional (P) or proportional-derivative (PD) controller. This type of linear controllers has been extensively used for CBC as it guarantees the existence of a noninvasive solution for $\xi^r(t)$. Therefore, it is thought that the iterative methods currently used to find noninvasive reference signals in CBC will also work for the adaptive control strategy proposed in this paper. However, contrary to using P and PD controllers directly on nonlinear systems (as in the literature), the proposed adaptive control strategy has a “guaranteed stabilizing performance”. Indeed, the surface $\mathbf{y}(t) = \mathbf{0}_p$ does not depend on unknown parameters, and the effect of all the unknown parameters is compensated for when $\lim_{t \rightarrow \infty} \mathbf{y}(t) = \mathbf{0}_p$. As long as $\mathbf{y}(t) = \mathbf{0}_p$, the tracking error $\mathbf{e}(t)$ converges to zero.

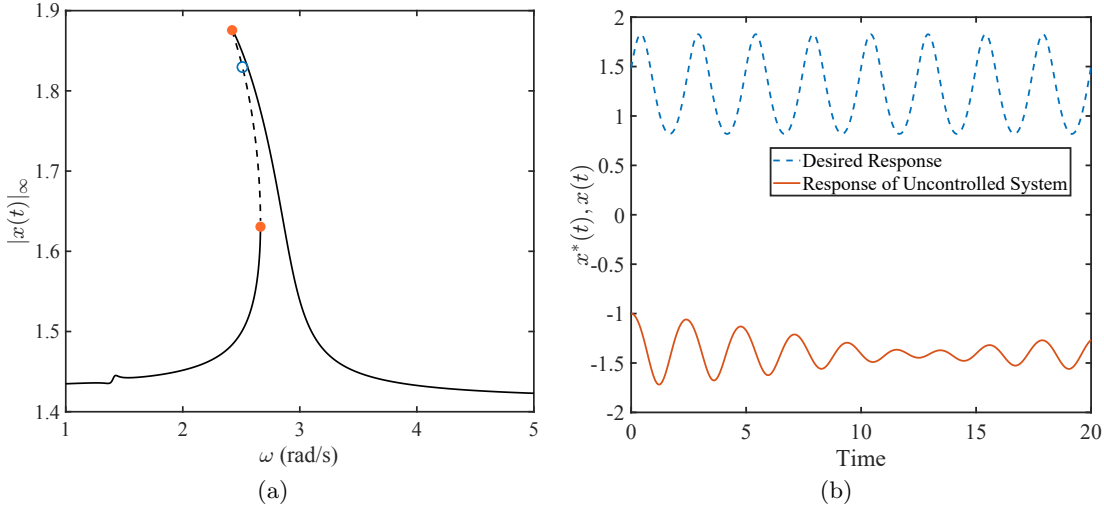


Figure 1. (a) Frequency response of the oscillator around the positive equilibrium in which the specific point associated with $\xi^*(t)$ is shown by a circle (\circ). The dashed line represents unstable responses, and dots (\bullet) show a limit-point bifurcation. (b) Desired responses of the uncontrolled oscillator for the initial states $(\dot{x}(0), x(0)) = (1.314, 1.483)$ and the uncontrolled response for the initial states $(\dot{x}(0), x(0)) = (0, -1)$.

5. Simulation Results. In this section, the accuracy of the proposed control strategy is numerically demonstrated on three systems. First, a bi-stable Duffing oscillator and then two beam structures exhibiting 1:1 and 3:1 modal interactions, respectively, are considered.

5.1. Duffing oscillator. Consider a forced Duffing oscillator with the following dynamics:

$$\ddot{x}(t) = \theta_1 \dot{x}(t) + \theta_2 x(t) + \theta_3 x(t)^3 + \sigma(t) + u'(t),$$

where $x(t)$ denotes the displacement of the oscillator, $\sigma(t)$ is the applied excitation, $u'(t)$ is the control input, and $\theta_1 = -0.1$, $\theta_2 = 4$, and $\theta_3 = -2$ are unknown damping, linear stiffness, and nonlinear stiffness parameters, respectively. For illustration, the response of the oscillator under harmonic excitation $\sigma(t) = 0.15 \cos(\omega t)$ is computed using numerical continuation and shown in Fig. 1-(a).

To illustrate the performance of the proposed control method, a reference signal corresponding to an unstable periodic response of the oscillator at $\omega = 2.515$ is chosen (see the circle marker in Fig. 1-(a)). This reference trajectory is given by $\xi^r(t) = \xi^*(t) = [\dot{x}^*(t) \quad x^*(t)]^\top$ where

$$x^*(t) \approx 1.271 + 0.244 \sin(\omega t) - 0.026 \sin(2\omega t) - 0.005 \sin(3\omega t) + 0.436 \cos(\omega t) + 0.045 \cos(2\omega t),$$

and $\dot{x}^*(t)$ is obtained by differentiating $x^*(t)$, and hence $(\dot{x}(0), x(0)) = (1.314, 1.483)$. The response of the oscillator is very sensitive to the initial states as the oscillator has two equilibria with stable steady-state oscillations around each. The desired response of the oscillator to $\sigma(t) = 0.15 \cos(\omega t)$ along with the response of the oscillator to $\sigma(t) = 0.15 \cos(\omega t)$ for the different initial states $(\dot{x}(0), x(0)) = (0, -1)$ is shown in Fig. 1-(b). Therefore, without control-

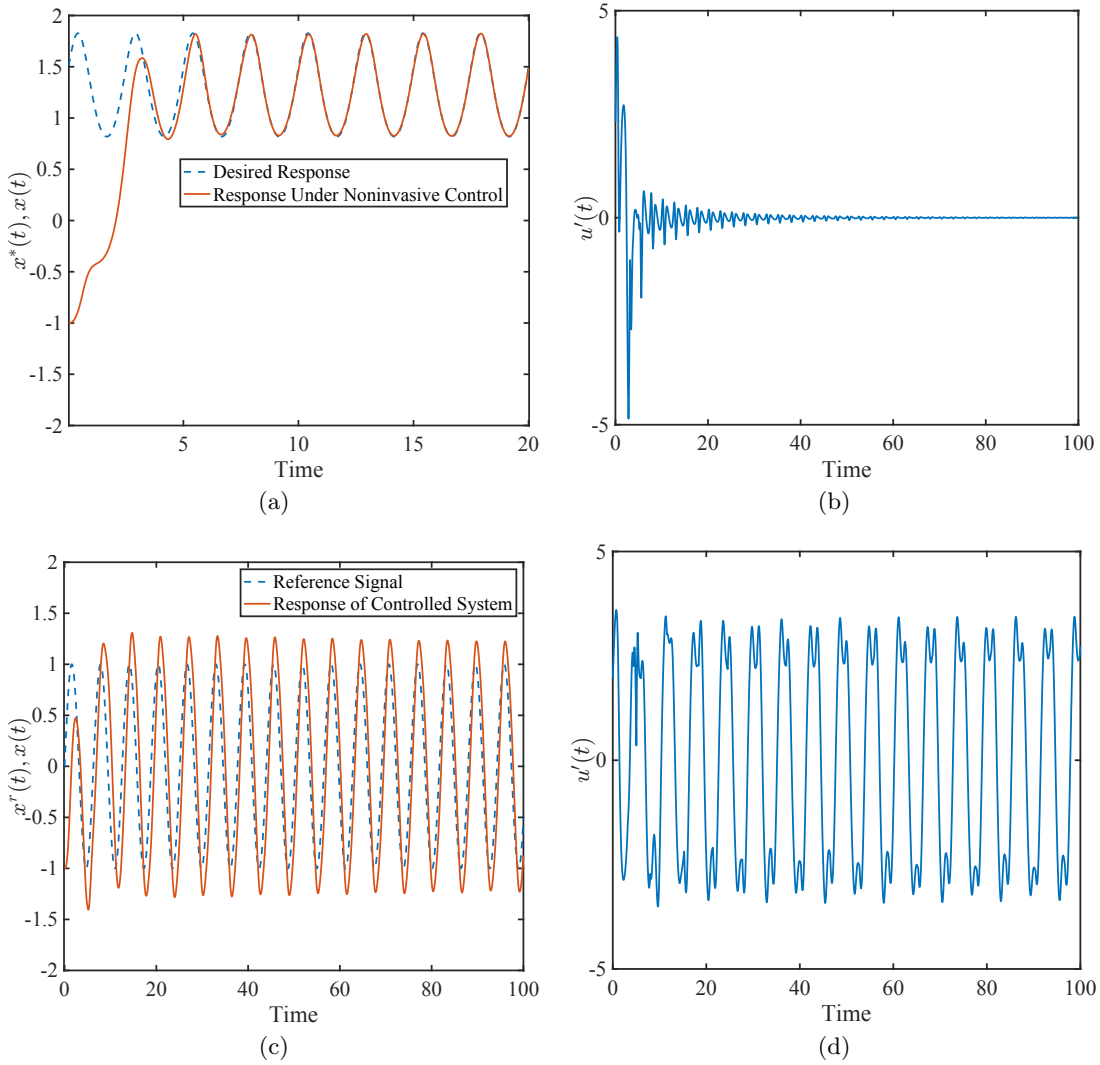


Figure 2. (a) Desired response of the oscillator with the initial states $(\dot{x}(0), x(0)) = (1.314, 1.483)$ and the controlled response of the oscillator for the initial states $(\dot{x}(0), x(0)) = (0, -1)$. (b) Noninvasive control input of the oscillator. (c) Desired reference $x^r(t) = \sin(t)$ (which is not a response to $\sigma(t)$) and controlled response of the oscillator. (d) Invasive control input of the oscillator when $\xi^r(t)$ is not a response to $\sigma(t)$.

based correction of the oscillator response, it is apparent that the oscillator response can be significantly different from the desired one. Note that $x^*(t)$ is an unstable trajectory of the uncontrolled oscillator. Therefore, it may not be precisely revealed even if the initial states of the oscillator are close to the initial states of the desired trajectory. By employing the proposed adaptive control strategy, it is guaranteed that the system response asymptotically converges to the desired response (see Fig. 2-(a)) while the control input asymptotically converges to zero, i.e., it becomes noninvasive (see Fig. 2-(b)). The control parameters used to obtain these results are $\mathbf{S} = 2\mathbf{I}_3$, $k = 1$, $\kappa = 1$, $\lambda_1 = 1$, $\gamma = 0.1$, and $\epsilon = 1$. Note that, depending on the

application, the control gains can be adjusted to reduce or increase control efforts. Smaller control efforts are usually associated with longer times for convergence of the states to the reference signal.

Under the proposed control strategy, $\boldsymbol{\xi}(t)$ does not converge to $\boldsymbol{\xi}^r(t)$ and $u'(t)$ is invasive if $\boldsymbol{\xi}^r(t)$ is not a response of the uncontrolled oscillator to $\sigma(t)$. To illustrate this, a control-based simulation is performed for an arbitrary reference signal defined as $x^r(t) = \sin(t)$. The system response and control input are shown in Fig. 2-(c) and Fig. 2-(d), respectively. As expected, $\boldsymbol{\xi}(t)$ does not converge to $\boldsymbol{\xi}^r(t)$ and $u'(t)$ is invasive.

5.2. Cross-beam structure. The cross-beam structure studied in [44] and inspired by the physical system tested in [15] is now considered. This structure has the particularity of having its first two vibration modes very close in frequency (0.5 Hz apart), leading to 1:1 mode interactions. As such, the model of the structure is a two degrees-of-freedom modal model given by

$$\ddot{\mathbf{x}}(t) + \boldsymbol{\Xi}\dot{\mathbf{x}}(t) + \mathbf{A}\mathbf{x}(t) + \mathbf{N}(\mathbf{x}(t)) = \boldsymbol{\sigma}(t) + \mathbf{u}'(t),$$

with

$$\begin{aligned} \mathbf{x}(t) &= \begin{bmatrix} x_1(t) \\ x_2(t) \end{bmatrix}, \boldsymbol{\Xi} = \begin{bmatrix} 2\zeta_1\omega_1 & 0 \\ 0 & 2\zeta_2\omega_2 \end{bmatrix}, \mathbf{A} = \begin{bmatrix} \omega_1^2 & 0 \\ 0 & \omega_2^2 \end{bmatrix}, \mathbf{N}(\mathbf{x}(t)) = \begin{bmatrix} \mathbf{N}_1(\mathbf{x}(t)) \\ \mathbf{N}_2(\mathbf{x}(t)) \end{bmatrix} \\ \mathbf{N}_1(\mathbf{x}(t)) &= 1/2\gamma_{11}x_1(t)^2 + 1/2(\gamma_{21} + \gamma_{31})x_1(t)x_2(t) + 1/2\gamma_{41}x_2(t)^2 + 1/3\gamma_{51}x_1(t)^3 \\ &\quad + 1/3(\gamma_{61} + \gamma_{71})x_1(t)x_2(t)^2 + 1/3(\gamma_{81} + \gamma_{91})x_1(t)^2x_2(t) + 1/3\gamma_{10,1}x_2(t)^3 \\ \mathbf{N}_2(\mathbf{x}(t)) &= 1/2\gamma_{12}x_1(t)^2 + 1/2(\gamma_{22} + \gamma_{32})x_1(t)x_2(t) + 1/2\gamma_{42}x_2(t)^2 + 1/3\gamma_{52}x_1(t)^3 \\ &\quad + 1/3(\gamma_{62} + \gamma_{72})x_1(t)x_2(t)^2 + 1/3(\gamma_{82} + \gamma_{92})x_1(t)^2x_2(t) + 1/3\gamma_{10,2}x_2(t)^3, \end{aligned}$$

where $x_1(t)$ and $x_2(t)$ denote the displacements of the first and second modes, respectively, ζ_1 and ζ_2 denote the linear damping ratios, ω_1 and ω_2 denote the natural frequencies which here are assumed to be unknown, and $\gamma_{ij}, i \in \{1, 2, \dots, 10\}, i \in \{1, 2\}$, are the unknown parameters of the nonlinear term $\mathbf{N}(\mathbf{x}(t))$. It is worth mentioning that such a model can describe a wide range of mechanical structures with geometric nonlinearity, and is therefore not limited to the cross-beam example considered here.

For the cross-beam system, the unknown parameters are set as $\zeta_1 = 0.0076$, $\zeta_2 = 0.0026$, $\omega_1 = 101.6$, $\omega_2 = 104.6$, $\gamma_{11} = 113.321$, $\gamma_{21} = -104.755$, $\gamma_{31} = -104.755$, $\gamma_{41} = -29.740$, $\gamma_{51} = 3.836 \times 10^8$, $\gamma_{61} = 2.451 \times 10^7$, $\gamma_{71} = 4.902 \times 10^7$, $\gamma_{81} = 1.929 \times 10^8$, $\gamma_{91} = 9.644 \times 10^7$, $\gamma_{10,1} = 6.104 \times 10^6$, $\gamma_{12} = -104.755$, $\gamma_{22} = -29.740$, $\gamma_{32} = -29.740$, $\gamma_{42} = 85.367$, $\gamma_{52} = 9.644 \times 10^7$, $\gamma_{62} = 6.104 \times 10^6$, $\gamma_{72} = 1.221 \times 10^7$, $\gamma_{82} = 4.902 \times 10^7$, $\gamma_{92} = 2.451 \times 10^7$, and $\gamma_{10,2} = 2.351 \times 10^6$. The frequency response of the structure for the first mode under the excitation $\boldsymbol{\sigma}(t) = [1.261 \cos(\omega t) \ 0.318 \cos(\omega t)]^\top$ is computed using numerical continuation and shown in Fig. 3.

To demonstrate the control method, we consider a reference signal $\boldsymbol{\xi}^r(t) = \boldsymbol{\xi}^*(t) = [\dot{x}_1^*(t) \ \dot{x}_2^*(t) \ x_1^*(t) \ x_2^*(t)]^\top$ which is an unstable response of the structure to $\boldsymbol{\sigma}(t)$ at $\omega = 118.814$ (see the circle marker in Fig. 3). This reference/desired response can be approximated

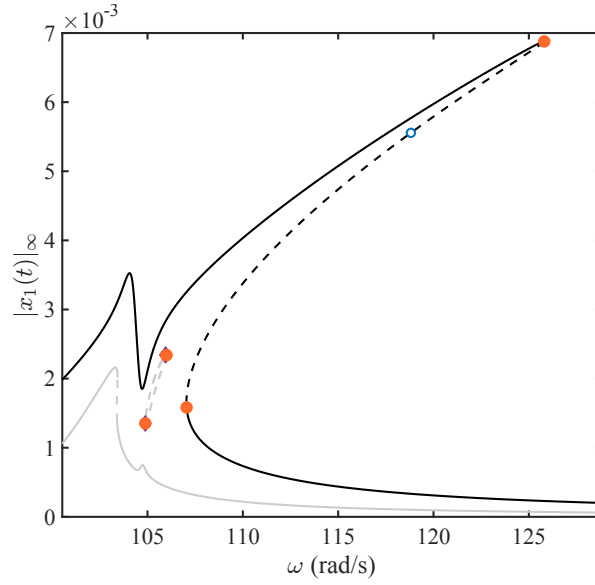


Figure 3. Frequency response curve associated with the first mode of the cross-beam structure. The specific point associated with $\xi^*(t)$ is shown by a circle (\circ), the dashed line represents unstable responses, and dots (\bullet) and diamonds (\blacklozenge) show limit-point and Neimark-Sacker bifurcations, respectively.

as

$$\begin{aligned} x_1^*(t) &\approx 10^{-4} \times (-35.344 \cos(\omega t) + 0.521 \cos(3\omega t) + 0.002 \cos(5\omega t) \\ &\quad + 42.08 \sin(\omega t) + 0.303 \sin(3\omega t) - 0.006 \sin(5\omega t)) \\ x_2^*(t) &\approx 10^{-4} \times (-10.974 \cos(\omega t) + 0.132 \cos(3\omega t) + 0.001 \cos(5\omega t) \\ &\quad + 12.358 \sin(\omega t) + 0.077 \sin(3\omega t) - 0.002 \sin(5\omega t)), \end{aligned}$$

and hence the initial states associated with this response are

$$(\dot{x}_1^*(0), \dot{x}_2^*(0), x_1^*(0), x_2^*(0)) = (0.5104, 0.1495, -0.0035, -0.0011).$$

To achieve the desired response, we employ the proposed adaptive control strategy with $\mathbf{S} = 2 \times 10^4 \mathbf{I}_{18}$, $k = 10^{-4}$, $\kappa = 10^{-4}$, $\lambda_1 = 10^{-4}$, $\gamma = 10^3$, and $\epsilon = 1$. The obtained response and control inputs are presented in Fig. 4. According to the figures, the system response asymptotically converges to the desired response and the control input is noninvasive.

The proposed control strategy assumes the knowledge of the function $\mathbf{F}(\boldsymbol{\xi}(t))$. Simulations show that the proposed control strategy has some robustness in the presence of some uncertainties in $\mathbf{F}(\boldsymbol{\xi}(t))$. To show this, we consider the case where all the cross terms $x_1(t)x_2(t)$, $x_1(t)x_2(t)^2$, and $x_1(t)^2x_2(t)$ are overlooked in the controller (4.1)-(4.8) whilst they are still present in the true system model. Simulation results show that the controller can still track the desired reference and achieve noninvasive control input (Fig. 5). In this example, as the reference signal $\boldsymbol{\xi}^r(t)$ satisfies the true dynamical model of the uncontrolled system, by convergence of $\boldsymbol{\xi}(t)$ to $\boldsymbol{\xi}^r(t)$, the effect of the missed terms is compensated. This example illustrates that the tracking of a desired reference signal and the noninvasiveness of the control input

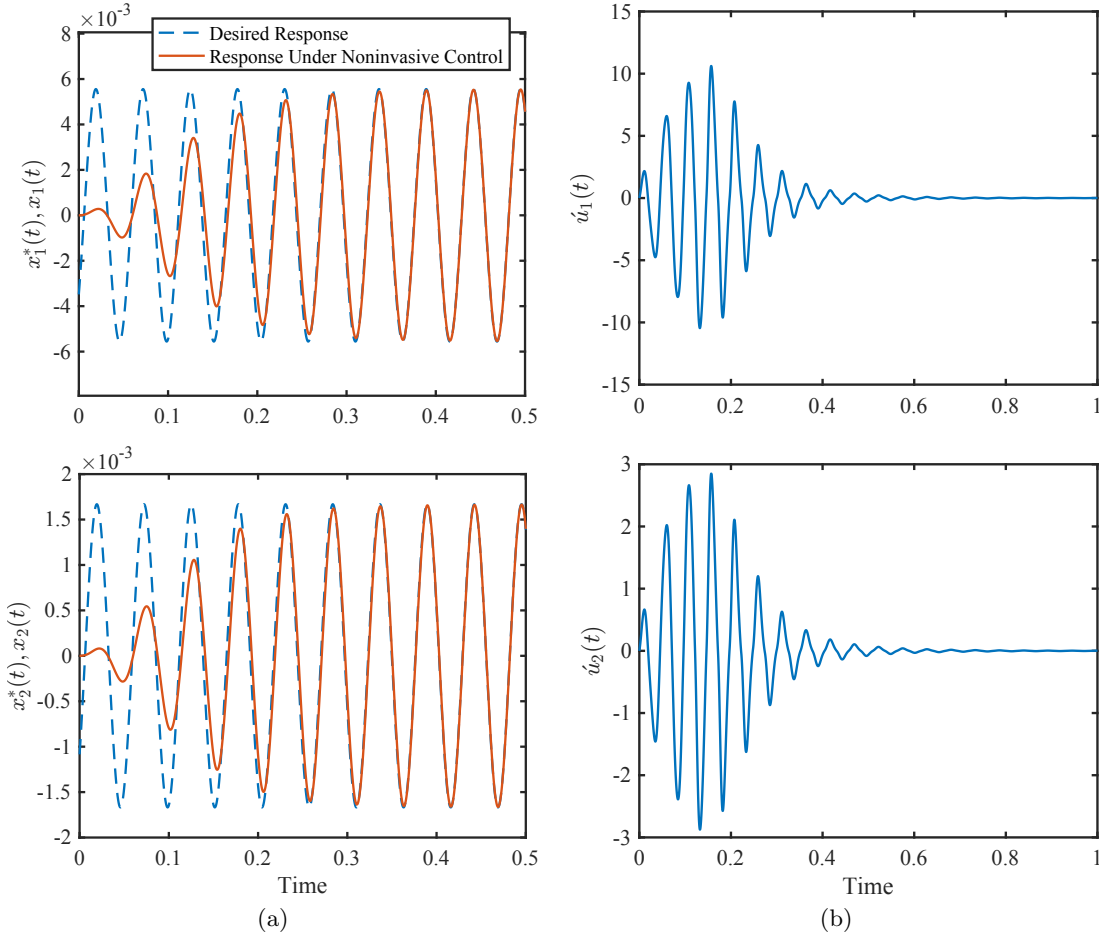


Figure 4. (a) Desired response of the cross-beam structure with the initial states $(\dot{x}_1(0), \dot{x}_2(0), x_1(0), x_2(0)) = (0.5104, 0.1495, -0.0035, -0.0011)$ and the controlled response of the cross-beam structure for the initial states $(\dot{x}_1(0), \dot{x}_2(0), x_1(0), x_2(0)) = (0, 0, 0, 0)$. (b) Noninvasive control inputs of the cross-beam structure.

can be obtained in the presence of model uncertainty provided the missed terms are not too large to be destabilizing. However, in general, it is always possible to find nonlinear terms that would lead to an unstable controlled system if not considered in the controller design (i.e., included in the true system model but not in the controller).

5.3. Cantilever beam with a nonlinear mechanism at its tip. A cantilever beam structure with nonlinear springs attached at its free end is now considered. This structure has the particularity to exhibit a 1:3 mode interaction between its first and second bending modes [50]. The system can be described by the following modal equations:

$$\ddot{\mathbf{x}}(t) + \mathbf{\Xi}\dot{\mathbf{x}}(t) + \mathbf{\Lambda}\mathbf{x}(t) + \mathbf{\Phi}^\top \mathbf{f}(\mathbf{\Phi}\mathbf{x}(t)) = \mathbf{\Phi}^\top \mathbf{u}(t),$$

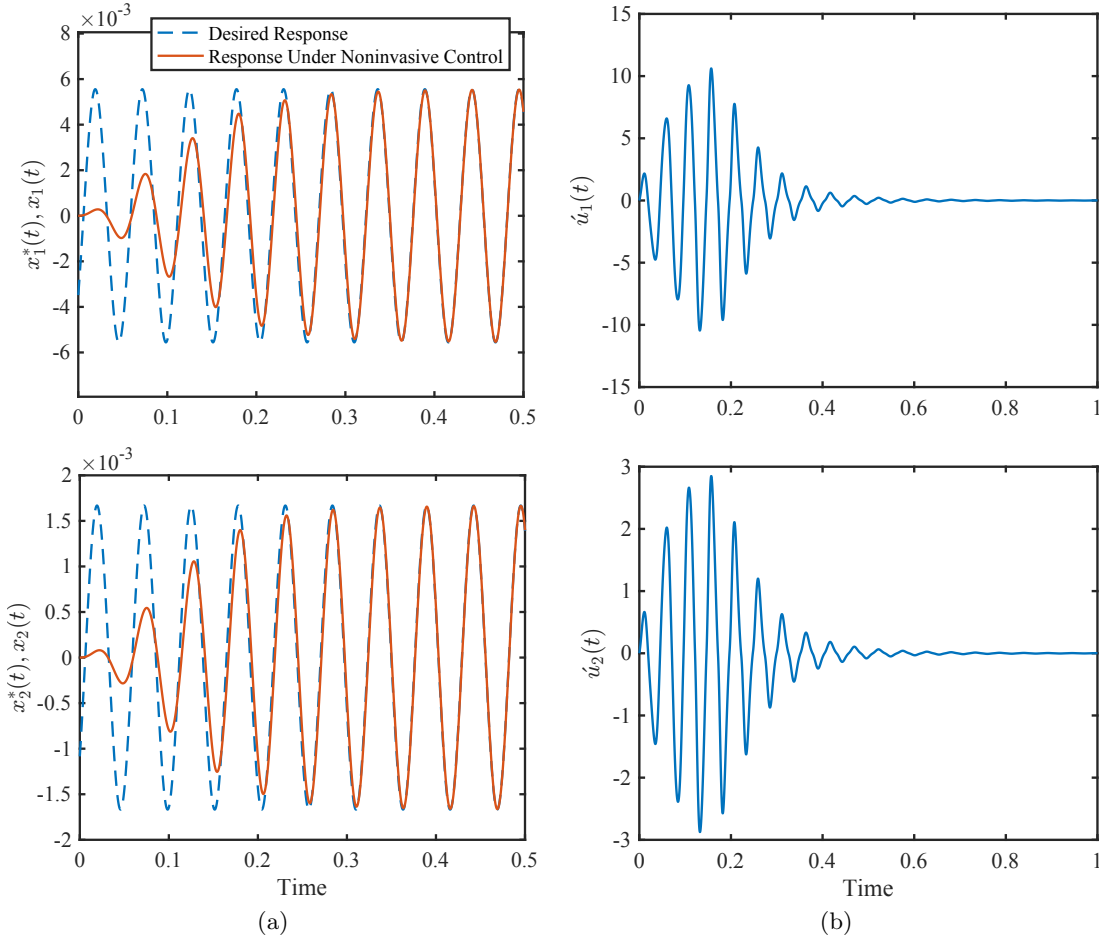


Figure 5. (a) Desired response of the cross-beam structure with the initial states $(\dot{x}_1(0), \dot{x}_2(0), x_1(0), x_2(0)) = (0.5104, 0.1495, -0.0035, -0.0011)$ and the controlled response of the cross-beam structure for the initial states $(\dot{x}_1(0), \dot{x}_2(0), x_1(0), x_2(0)) = (0, 0, 0, 0)$, when the model nonlinearities are partially unknown. (b) Noninvasive control inputs of the cross-beam structure, when the model nonlinearities are partially unknown.

with

$$(5.1) \quad \mathbf{x}(t) = \begin{bmatrix} x_1(t) \\ x_2(t) \end{bmatrix}, \mathbf{\Xi} = \begin{bmatrix} 2\zeta_1\omega_1 & 0 \\ 0 & 2\zeta_2\omega_2 \end{bmatrix}, \mathbf{A} = \begin{bmatrix} \omega_1^2 & 0 \\ 0 & \omega_2^2 \end{bmatrix}$$

$$\mathbf{f}(\Phi\mathbf{x}(t)) = \begin{bmatrix} 0 & 0 & 0 & 2k_0\ell_0x'_4 \left(\frac{1}{a} - \frac{1}{\sqrt{a^2 + x'_4(t)^2}} \right) \end{bmatrix}^\top, \mathbf{u}(t) = [u_1(t) \quad u_2(t) \quad 0 \quad 0]^\top$$

$$\Phi\mathbf{x}(t) = [x'_1(t) \quad x'_2(t) \quad x'_3(t) \quad x'_4(t)]^\top = \mathbf{x}'(t),$$

where $x_1(t)$, $x_2(t)$, ζ_1 , ζ_2 , ω_1 , and ω_2 have the same meaning as in Section 5.2, k_0 is the stiffness coefficient of the springs, ℓ_0 is their original length, a is the half span of the mechanism, and $\Phi \in \mathbb{R}^{4 \times 2}$ describes the relation between the modal variables and the physical deflection of the

beam at four specific points along the beam denoted by $\mathbf{x}'(t)$. For this system, the parameters are $\zeta_1 = 0.01$, $\zeta_2 = 0.01$, $\omega_1 = 67.395$, $\omega_2 = 235.783$, $k_0 = 910$, $\ell_0 = 0.018$, $a = 0.019$, and

$$\Phi = \begin{bmatrix} -0.1603 & -0.6821 \\ -1.7748 & -4.4598 \\ -5.9745 & 6.1940 \\ -6.1389 & 7.0245 \end{bmatrix}.$$

To describe (5.1) with the model class (3.1), the mode shape matrix Φ is assumed to be known, which in practice can be achieved using standard linear system identification techniques. All the other model parameters are considered unknown. Moreover, since the system has two degrees-of-freedom, we assumed we have two control inputs. The response of the structure for the first mode under the excitation $\sigma(t) = [2 \cos(\omega t) \ 0 \ 0 \ 0]^\top$ is computed using numerical continuation and shown in Fig. 6.

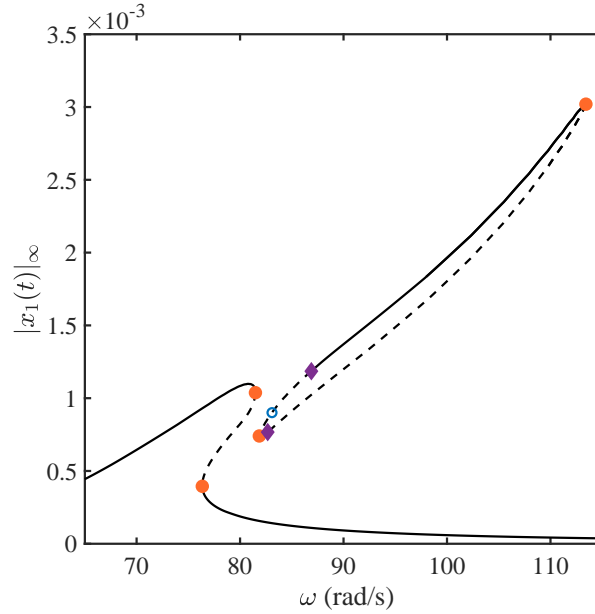


Figure 6. Frequency response associated with the first mode of the cantilever beam structure. The specific point associated with $\xi^*(t)$ is shown by a circle (o), the dashed line represents unstable responses, and dots (o) and diamonds (diamond) show limit-point and Neimark-Sacker bifurcations, respectively.

A reference signal $\xi^r(t) = \xi^*(t) = [x_1^*(t) \ \dot{x}_2^*(t) \ x_1^*(t) \ x_2^*(t)]^\top$ is considered to be an unstable response of the beam structure to $\sigma(t)$ when $\omega = 83.085$ (see the circle marker in Fig. 6). This reference/desired response can be approximated as

$$\begin{aligned} x_1^*(t) &\approx 10^{-4} \times (-2.834 \cos(\omega t) + 0.254 \cos(3\omega t) - 0.0341 \cos(5\omega t) - 0.001 \cos(7\omega t) \\ &\quad - 8.241 \sin(\omega t) + 0.066 \sin(3\omega t) + 0.026 \sin(5\omega t) - 0.007 \sin(7\omega t)) \\ x_2^*(t) &\approx 10^{-4} \times (-0.487 \cos(\omega t) - 2.6 \cos(3\omega t) + 0.055 \cos(5\omega t) + 0.001 \cos(7\omega t) \\ &\quad - 0.469 \sin(\omega t) - 0.219 \sin(3\omega t) - 0.044 \sin(5\omega t) + 0.009 \sin(7\omega t)), \end{aligned}$$

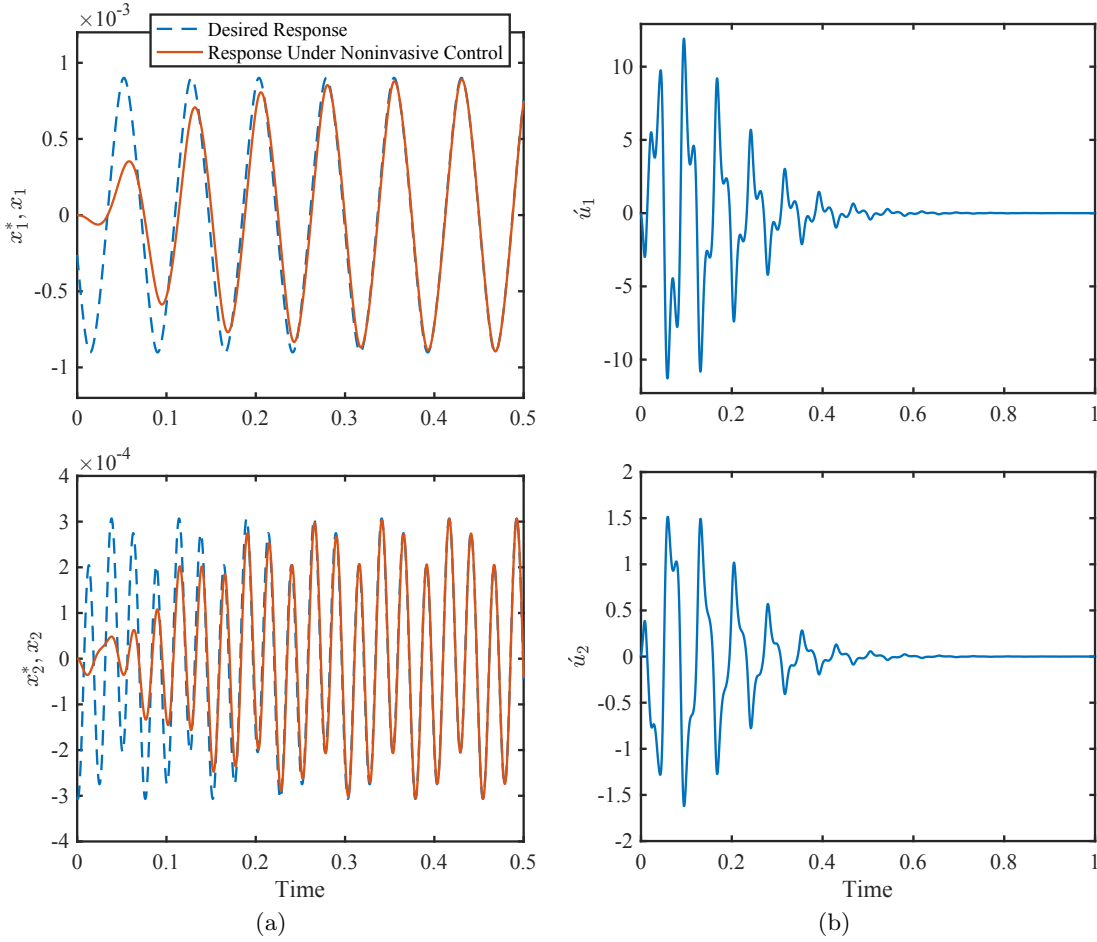


Figure 7. (a) Desired response of the cantilever beam structure with the initial states $(\dot{x}_1(0), \dot{x}_2(0), x_1(0), x_2(0)) = (-0.066, -0.011, -2.613 \times 10^{-4}, -3.031 \times 10^{-4})$ and the controlled response of the cantilever beam structure for the initial states $(\dot{x}_1(0), \dot{x}_2(0), x_1(0), x_2(0)) = (0, 0, 0, 0)$. (b) Noninvasive control inputs of the cantilever beam structure.

and hence the initial states associated with this response are

$$(\dot{x}_1(0), \dot{x}_2(0), x_1(0), x_2(0)) = (-0.066, -0.011, -2.613 \times 10^{-4}, -3.031 \times 10^{-4}).$$

To achieve the desired response $\xi^*(t)$, we employ the proposed adaptive control strategy with $\mathbf{S} = 2 \times 10^5 \mathbf{I}_{18}$, $k = 10^{-4}$, $\kappa = 10^{-4}$, $\lambda_1 = 10^{-4}$, $\gamma = 10^5$, and $\epsilon = 1$. The simulation results, presented in Fig. 7-(a), show that the system response asymptotically converges to the desired one. As shown in Fig. 7-(b), the control input becomes noninvasive as the system reaches the desired response.

One of the contributions of the paper is that contrary to the existing literature, the noninvasiveness of the proposed control strategy does not rely on the true estimation of the system parameters and thereby does not rely on the persistent excitation of the desired response. To show this, the norm of the estimation error $\hat{\theta}(t) = \hat{\theta}(t) - \theta$ when $\hat{\theta}(t)$ is initialized to zero and

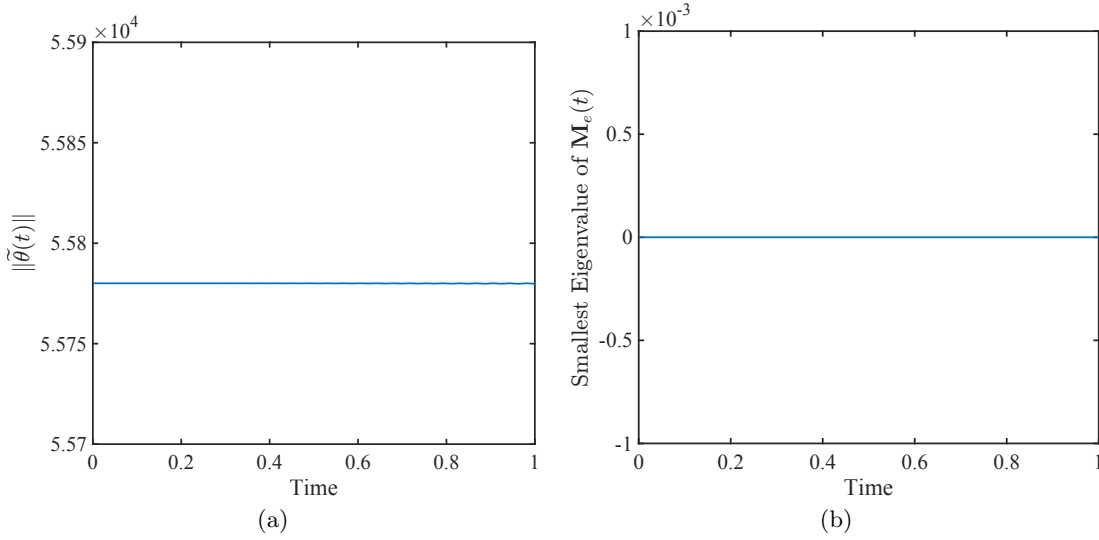


Figure 8. (a) Error of estimating the parameters of the cantilever beam structure. (b) The smallest eigenvalue of the matrix $M_e(t)$ associated with the cantilever beam structure.

$\|\theta\| = 5.578 \times 10^4$ is shown in Fig. 8-(a). According to the figure, the estimation error does not converge to zero, and a negligible update in the model parameters $\hat{\theta}(t)$ occurs. Defining the matrix

$$M_e(t) = \int_t^{t+s} \mathbf{F}(\xi(\tau))^\top \mathbf{F}(\xi(\tau)) d\tau,$$

the persistent excitation condition is satisfied if $M_e(t)$, $t \rightarrow \infty$, is positive definite, i.e., its smallest eigenvalue is positive, for some real positive constant s (s can be the time period in the case of periodic response). The smallest eigenvalue of $M_e(t)$ along the system trajectory is shown in Fig. 8-(b), which stays at zero and illustrates that $M_e(t)$ is not positive definite. Hence, the controlled system is not persistently excited along the system trajectory.

6. Conclusion and Future Work. Control-based continuation is an increasingly popular method to characterize the nonlinear dynamics of a physical system directly during tests, without the need for a model. Despite being successfully applied to a wide range of experiments and providing invaluable results for model calibration and validation, the general and systematic design of the noninvasive controller at the core of the method is lacking.

In this paper, an adaptive strategy for noninvasive control of nonlinear systems that are linear in their unknown parameters is proposed. The method guarantees the convergence to the desired response and the noninvasiveness of the control input if and only if the reference signal is a natural response of the uncontrolled system to the excitation force $\sigma(t)$. Compared to other available methods, the proposed control strategy does not require any knowledge of the system parameters nor their exact estimation, and it does not assume stable linearized dynamics. This makes the proposed methodology applicable to a much wider range of nonlinear systems, with a wider range of response types. Furthermore, the proposed method does

not rely on the persistence of the excitation, which, in the context of CBC, means there is no need to guarantee/check the persistent nature of the excitation during experiments for the noninvasiveness of the controller. This has the potential to increase CBC accuracy and reduce overall testing time.

REFERENCES

- [1] G. ABELOOS, F. MÜLLER, E. FERHATOGLU, M. SCHEEL, C. COLLETTE, G. KERSCHEN, M. BRAKE, P. TISO, L. RENSON, AND M. KRACK, *A consistency analysis of phase-locked-loop testing and control-based continuation for a geometrically nonlinear frictional system*, *Mechanical Systems and Signal Processing*, 170 (2022), <https://doi.org/10.1016/j.ymsp.2022.108820>.
- [2] G. ABELOOS, L. RENSON, C. COLLETTE, AND G. KERSCHEN, *Stepped and swept control-based continuation using adaptive filtering*, *Nonlinear Dynamics*, 104 (2021), pp. 3793–3808, <https://doi.org/10.1007/s11071-021-06506-z>.
- [3] I. BARKANA, *Defending the beauty of the Invariance Principle*, *International Journal of Control*, 87 (2014), pp. 186–206, <https://doi.org/10.1080/00207179.2013.826385>.
- [4] D. A. BARTON, B. P. MANN, AND S. G. BURROW, *Control-based continuation for investigating nonlinear experiments*, *Journal of Vibration and Control*, 18 (2012), pp. 509–520, <https://doi.org/10.1177/1077546310384004>.
- [5] D. A. W. BARTON AND J. SIEBER, *Systematic experimental exploration of bifurcations with noninvasive control*, *Physical Review E*, 87 (2013), <https://doi.org/10.1103/PhysRevE.87.052916>.
- [6] E. BENKLER, M. KREUZER, R. NEUBECKER, AND T. TSCHUDI, *Noninvasive experimental control of beam profiles in nonlinear optics*, *Journal of Optics A: Pure and Applied Optics*, 2 (2000), pp. 303–309, <https://doi.org/10.1088/1464-4258/2/4/311>.
- [7] S. BEREGI, D. BARTON, D. REZGUI, AND S. NEILD, *Using scientific machine learning for experimental bifurcation analysis of dynamic systems*, *Mechanical Systems and Signal Processing*, 184 (2023), <https://doi.org/10.1016/j.ymsp.2022.109649>.
- [8] S. BEREGI, D. A. W. BARTON, D. REZGUI, AND S. A. NEILD, *Robustness of nonlinear parameter identification in the presence of process noise using control-based continuation*, *Nonlinear Dynamics*, 104 (2021), pp. 885–900, <https://doi.org/10.1007/s11071-021-06347-w>.
- [9] M. BLYTH, K. TSANEVA-ATANASOVA, L. MARUCCI, AND L. RENSON, *Numerical methods for control-based continuation of relaxation oscillations*, *Nonlinear Dynamics*, 111 (2023), pp. 7975–7992, <https://doi.org/10.1007/s11071-023-08288-y>.
- [10] S. BOCCALETTI, C. GREBOGI, Y.-C. LAI, H. MANCINI, AND D. MAZA, *The control of chaos: theory and applications*, *Physics Reports*, 329 (2000), pp. 103–197, [https://doi.org/10.1016/S0370-1573\(99\)00096-4](https://doi.org/10.1016/S0370-1573(99)00096-4).
- [11] E. BUREAU, F. SCHILDER, I. FERREIRA SANTOS, J. JUEL THOMSEN, AND J. STARKE, *Experimental bifurcation analysis of an impact oscillator—Tuning a non-invasive control scheme*, *Journal of Sound and Vibration*, 332 (2013), pp. 5883–5897, <https://doi.org/10.1016/j.jsv.2013.05.033>.
- [12] I. DE CESARE, D. SALZANO, M. DI BERNARDO, L. RENSON, AND L. MARUCCI, *Control-based continuation: A new approach to prototype synthetic gene networks*, *ACS Synthetic Biology*, 11 (2022), pp. 2300–2313, <https://doi.org/10.1021/acssynbio.1c00632>.
- [13] V. DENIS, M. JOSSIC, C. GIRAUD-AUDINE, B. CHOMETTE, A. RENAULT, AND O. THOMAS, *Identification of nonlinear modes using phase-locked-loop experimental continuation and normal form*, *Mechanical Systems and Signal Processing*, 106 (2018), pp. 430–452, <https://doi.org/10.1016/j.ymsp.2018.01.014>.
- [14] A. DITTUS, N. KRUSE, I. BARKE, S. SPELLER, AND J. STARKE, *Detecting stability and bifurcation points in control-based continuation for a physical experiment of the Zeeman catastrophe machine*, *SIAM Journal on Applied Dynamical Systems*, 22 (2023), pp. 1275–1299, <https://doi.org/10.1137/22M150324>.
- [15] D. A. EHRHARDT, T. L. HILL, AND S. A. NEILD, *Experimentally measuring an isolated branch of nonlinear normal modes*, *Journal of Sound and Vibration*, 457 (2019), pp. 213–226, <https://doi.org/>

- 10.1016/j.jsv.2019.06.006.
- [16] V. FLUNKERT AND E. SCHÖLL, *Towards easier realization of time-delayed feedback control of odd-number orbits*, Physical Review E, 84 (2011), <https://doi.org/10.1103/PhysRevE.84.016214>.
 - [17] J. FONTANA AND A. THOMPSON, *Feedback control of propagating bubbles in Hele-Shaw channels*, in Proceedings of the 10th European Nonlinear Dynamics Conference, Lyon, France, July 2022.
 - [18] A. GARFINKEL, M. SPANO, W. DITTO, AND J. WEISS, *Controlling cardiac chaos*, Science, 257 (1992), pp. 1230–1235, <https://doi.org/10.1126/science.1519060>.
 - [19] J. GUCKENHEIMER, K. HOFFMAN, AND W. WECKESSER, *The forced van der Pol equation I: The slow flow and its bifurcations*, SIAM Journal on Applied Dynamical Systems, 2 (2003), pp. 1–35, <https://doi.org/10.1137/S1111111102404738>.
 - [20] S. HAYES, C. GREBOGI, E. OTT, AND A. MARK, *Experimental control of chaos for communication*, Physical Review Letters, 73 (1994), pp. 1781–1784, <https://doi.org/10.1103/PhysRevLett.73.1781>.
 - [21] P. HIPPOLD, M. SCHEEL, L. RENSON, AND M. KRACK, *Robust and fast backbone tracking via phase-locked loops*, Mechanical Systems and Signal Processing, 220 (2024), <https://doi.org/10.1016/j.ymssp.2024.111670>.
 - [22] W. JUST, *Synchronization of non-identical systems by non-invasive mutual time-delayed feedback*, Chaos: An Interdisciplinary Journal of Nonlinear Science, 33 (2023), <https://doi.org/10.1063/5.0142803>.
 - [23] H. K. KHALIL, *Nonlinear Control*, Prentice Hall, Upper Saddle River, New Jersey, USA, 3rd ed., 2002.
 - [24] G. KLEYMAN, M. PAEHR, AND S. TATZKO, *Application of control-based-continuation for characterization of dynamic systems with stiffness and friction nonlinearities*, Mechanics Research Communications, 106 (2020), <https://doi.org/10.1016/j.mechrescom.2020.103520>.
 - [25] K. LEE, D. BARTON, AND L. RENSON, *Modelling of physical systems with a Hopf bifurcation using mechanistic models and machine learning*, Mechanical Systems and Signal Processing, 191 (2023), <https://doi.org/10.1016/j.ymssp.2023.110173>.
 - [26] S. LENCI, *Exact solutions for coupled duffing oscillators*, Mechanical Systems and Signal Processing, 165 (2022), <https://doi.org/10.1016/j.ymssp.2021.108299>.
 - [27] Y. LI AND H. DANKOWICZ, *Adaptive control designs for control-based continuation in a class of uncertain discrete-time dynamical systems*, Journal of Vibration and Control, 26 (2020), pp. 2092–2109, <https://doi.org/10.1177/1077546320913377>.
 - [28] Y. LI AND H. DANKOWICZ, *Adaptive control designs for control-based continuation of periodic orbits in a class of uncertain linear systems*, Nonlinear Dynamics, 103 (2021), pp. 2563–2579, <https://doi.org/10.1007/s11071-021-06216-6>.
 - [29] Y. LI AND H. DANKOWICZ, *Model-free continuation of periodic orbits in certain nonlinear systems using continuous-time adaptive control*, Nonlinear Dynamics, 111 (2023), p. 4945–4957, <https://doi.org/10.1007/s11071-022-08059-1>.
 - [30] W.-G. LU, L.-W. ZHOU, Q.-M. LUO, AND X.-F. ZHANG, *Filter based non-invasive control of chaos in buck converter*, Physics Letters A, 372 (2008), pp. 3217–3222, <https://doi.org/10.1016/j.physleta.2008.01.042>.
 - [31] X. MA, D. XIA, W. JIANG, M. LIU, AND Q. BI, *Compound bursting behaviors in a forced Mathieu-van der Pol-Duffing system*, Chaos, Solitons & Fractals, 147 (2021), <https://doi.org/10.1016/j.chaos.2021.110967>.
 - [32] S. MOJRZISCH, J. WALLASCHEK, AND J. BREMER, *An experimental method for the phase controlled frequency response measurement of nonlinear vibration systems*, Proceedings of the Applied Mathematics and Mechanics, 12 (2012), pp. 253–254, <https://doi.org/10.1002/pamm.201210117>.
 - [33] R. NEVILLE, R. M. J. GROH, A. PIRRERA, AND M. SCHENK, *Shape control for experimental continuation*, Physical Review Letters, 120 (2018), <https://doi.org/10.1103/PhysRevLett.120.254101>.
 - [34] E. OTT, C. GREBOGI, AND J. A. YORKE, *Controlling chaos*, Physical Review Letters, 64 (1990), pp. 1196–1199, <https://doi.org/10.1103/PhysRevLett.64.1196>.
 - [35] I. PANAGIOTOPOULOS, J. STARKE, J. SIEBER, AND W. JUST, *Continuation with noninvasive control schemes: Revealing unstable states in a pedestrian evacuation scenario*, SIAM Journal on Applied Dynamical Systems, 22 (2023), pp. 1–36, <https://doi.org/10.1137/22M1482032>.
 - [36] B. PENG, V. PETROV, AND K. SHOWALTER, *Controlling chemical chaos*, The Journal of Physical Chemistry, 95 (1991), pp. 4957–4959, <https://doi.org/10.1021/j100166a013>.
 - [37] S. PETER AND R. I. LEINE, *Excitation power quantities in phase resonance testing of nonlinear systems*

- with phase-locked-loop excitation, *Mechanical Systems and Signal Processing*, 96 (2017), pp. 139–158, <https://doi.org/10.1016/j.ymssp.2017.04.011>.
- [38] V. PETROV, V. GÁSPÁR, J. MASERE, AND K. SHOWALTER, *Controlling chaos in the Belousov–Zhabotinsky reaction*, *Nature*, 361 (1993), pp. 240–243, <https://doi.org/10.1038/361240a0>.
- [39] K. PYRAGAS, *Continuous control of chaos by self-controlling feedback*, *Physics Letters A*, 170 (1992), pp. 421–428, [https://doi.org/10.1016/0375-9601\(92\)90745-8](https://doi.org/10.1016/0375-9601(92)90745-8).
- [40] T. PYRAGIENĖ, A. TAMAŠEVIČIUS, G. MYKOLAITIS, AND K. PYRAGAS, *Non-invasive control of synchronization region of a forced self-oscillator via a second order filter*, *Physics Letters A*, 361 (2007), pp. 323–331, <https://doi.org/10.1016/j.physleta.2006.09.072>.
- [41] G. REGA, S. LENCI, AND J. THOMPSON, *Controlling Chaos: The OGY Method, Its Use in Mechanics, and an Alternative Unified Framework for Control of Non-regular Dynamics*, Springer Berlin Heidelberg, Germany, 2010, pp. 211–269, https://doi.org/10.1007/978-3-642-04629-2_11.
- [42] L. RENSON, D. A. W. BARTON, AND S. A. NEILD, *Experimental tracking of limit-point bifurcations and backbone curves using control-based continuation*, *International Journal of Bifurcation and Chaos*, 27 (2017), <https://doi.org/10.1142/S0218127417300026>.
- [43] L. RENSON, A. GONZALEZ-BUELGA, D. BARTON, AND S. NEILD, *Robust identification of backbone curves using control-based continuation*, *Journal of Sound and Vibration*, 367 (2016), pp. 145–158, <https://doi.org/10.1016/j.jsv.2015.12.035>.
- [44] L. RENSON, T. L. HILL, D. A. EHRHARDT, D. A. W. BARTON, AND S. A. NEILD, *Force appropriation of nonlinear structures*, *Proceedings of the Royal Society A*, 474 (2018), <https://doi.org/10.1098/rspa.2017.0880>.
- [45] L. RENSON, J. SIEBER, D. BARTON, A. SHAW, AND S. NEILD, *Numerical continuation in nonlinear experiments using local Gaussian process regression*, *Nonlinear Dynamics*, 98 (2019), pp. 2811–2826, <https://doi.org/10.1007/s11071-019-05118-y>.
- [46] T. S. RICHARDSON AND M. H. LOWENBERG, *A continuation design framework for nonlinear flight control problems*, *The Aeronautical Journal*, 110 (2006), pp. 85–96, <https://doi.org/10.1017/S000192400001032>.
- [47] S. SCHIKORA, H.-J. WÜNSCHE, AND F. HENNEBERGER, *All-optical noninvasive chaos control of a semiconductor laser*, *Physical Review E*, 78 (2008), <https://doi.org/10.1103/physreve.78.025202>.
- [48] F. SCHILDER, E. BUREAU, I. F. SANTOS, J. J. THOMSEN, AND J. STARKE, *Experimental bifurcation analysis—continuation for noise-contaminated zero problems*, *Journal of Sound and Vibration*, 358 (2015), pp. 251–266, <https://doi.org/10.1016/j.jsv.2015.08.008>.
- [49] E. SCHÖLL AND H. G. SCHUSTER, *Handbook of Chaos Control*, Wiley-VCH, Weinheim, Germany, 2nd ed., 2007, <https://doi.org/10.1002/9783527622313.fmatter>.
- [50] A. D. SHAW, T. L. HILL, S. A. NEILD, AND M. I. FRISWELL, *Periodic responses of a structure with 3:1 internal resonance*, *Mechanical Systems and Signal Processing*, 81 (2016), pp. 19–34, <https://doi.org/10.1016/j.ymssp.2016.03.008>.
- [51] J. SHEN, R. GROH, M. SCHENK, AND A. PIRRERA, *Experimental path-following of equilibria using Newton’s method. Part I: Theory, modelling, experiments*, *International Journal of Solids and Structures*, 210–211 (2021), pp. 203–223, <https://doi.org/10.1016/j.ijsolstr.2020.11.037>.
- [52] J. SHEN, R. GROH, M. SCHENK, AND A. PIRRERA, *Experimental path-following of equilibria using Newton’s method. Part II: Applications and outlook*, *International Journal of Solids and Structures*, 213 (2021), pp. 25–40, <https://doi.org/10.1016/j.ijsolstr.2020.11.038>.
- [53] J. SIEBER AND B. KRAUSKOPF, *Control based bifurcation analysis for experiments*, *Nonlinear Dynamics*, 51 (2008), pp. 365–377, <https://doi.org/10.1007/s11071-007-9217-2>.
- [54] J. SINGER AND H. BAU, *Active control of convection*, *Physics of Fluids*, 3 (1991), pp. 2859–2865, <https://doi.org/10.1063/1.857831>.
- [55] M. SONG, L. RENSON, B. MOAVENI, AND G. KERSCHEN, *Bayesian model updating and class selection of a wing-engine structure with nonlinear connections using nonlinear normal modes*, *Mechanical Systems and Signal Processing*, 165 (2022), <https://doi.org/10.1016/j.ymssp.2021.108337>.
- [56] G. TAO, *A simple alternative to the Barbalat lemma*, *IEEE Transactions on Automatic Control*, 42 (1997), p. 698, <https://doi.org/10.1109/9.580878>.